MnDOT Contract No.1003326 WO 2

NRRA LT1: Developing Best Practices for Rehabilitation of Concrete with Hot Mix Asphalt (HMA) Overlays related to Density and Reflective Cracking

Task -2: Gathering Past Performance Data and Laboratory Testing

Task Memo

Prepared by:

Katie E. Haslett, Eshan V. Dave, and Jo E. Sias

Department of Civil and Environmental Engineering, University of New Hampshire

August 2019

Published by:
Minnesota Department of Transportation
Research Services Section
395 John Ireland Boulevard, MS 330
St. Paul, Minnesota 55155-1899

Table of Contents

List of Tables

List of Figures

1. Introduction

Task-2 of the "Developing Best Practices for Rehabilitation of Concrete with Hot Mix Asphalt (HMA) Overlays related to Density and Reflective Cracking," project was focused on gathering past performance data and laboratory testing. This report summaries field performance data collected from 12 MnROAD test sections in addition to a variety of laboratory performed tests on those mixtures to characterize mix performance. Statistical comparison of lab performance, field performance and mixture volumetric properties was completed as part of this task. Results of an agency survey that was developed by the research team and distributed to all NRRA state members in an effort to collect information on current and past performance data of overlays on PCC pavements is also summarized in this report.

A brief summary of the laboratory testing partners, mixtures and corresponding field sections evaluated as part of the fulfillment of Task-2 is presented in Table 1, Table 2 and Table 3 respectively.

Table 1: Laboratory testing partners.

Laboratory Test	Agency/Lab
Disk-shaped Compact Tension (DCT)	MnDOT
AASHTO T-283 TSR	MODOT
I-FIT (SCB)	IDOT
Texas Overlay Tester (OT)	IDOT
Hamburg Wheel Tracking Tester	WisDOT
Moisture Induced Stress Tester (MiST)	MTU
Indirect tensile Strength and Creep (IDT)	MnDOT
Dynamic Modulus (E*)	UNH
Direct Tension Cyclic Fatigue (S-VECD)	UNH
Compact Tension (CT)	UNH

Table 2: Summary of mixtures being evaluated.

Mix ID	NMAS	Binder	Des. Air Voids	Des. Total AC (%)	Rap (%)	Des. Gyrations
SPWEA440E	9.5	58H-28	4.0	5.8	25	90
SPWEB340C	12.5	58H-34	4.0	5.3	10	60
SPWEB430E	12.5	58H-28	3.0	5.7	20	90
SPWEB440E	12.5	58H-28	4.0	5.4	20	90
SPWEB450E	12.5	58H-28	5.0	6.6	15	50
SPWEC440E	19.0	58H-28	4.0	5.6	10	90
SPWED430I	4.75	58E-34	2.0-3.0	8.2	0	50
SPWED440E	4.75	58H-28	4.0	7.0	0	75
UTBWC	-	58V-34	-	5.3	0	-

Table 3: Summary of mixtures and field sections at MnROAD.

Cell	Roadway	Experiment	Description	Mixture Type	MDR	Comment	Thickness (in)
983	I-94 WB	HMA Rehab	Control section	N.A	-	-	-
984			HMA over concrete (1 lift)	SPWEA440E	2017-168	Single lift	1.5
985				SPWEB440E	2017-169	Single lift	1.5
986				SPWEB440E	2017-169	Single lift + Spray Paver	1.75
987			HMA over concrete (2 lift)	SPWEC440E	2017-105	Lift 1	2.5
				SPWEA440E	2017-168	Lift 2	1.5
988		Compaction Study	HMA over concrete (2 lift)	SPWEC440E	2017-105	Lift 1	2.25
				SPWEB440E	2017-169	Lift 2	1.75
989				SPWEC440E	2017-105	Lift 1	2.25
				SPWEB450E	2017-125	Lift 2	1.75
990				SPWEC440E	2017-105	Lift 1	2.25
				SPWEB430E	2017-170	Lift 2	1.75
991				SPWEC440E	2017-105	Lift 1	2.25
				SPWEA440E	2017-168	Lift 2	1.75
992		HMA Rehab	HMA over concrete w/ interlayer	SPWED430I	2017-149	Lift 1 (interlayer)	1
				SPWEA440E	2017-168	Lift 2 (over interlayer)	1.5
993			HMA over concrete w/ PASSRC	PASSRC	2017-080	Lift 1	1
				SPWEA440E	2017-168	Lift 2	1.5
994			HMA over concrete (1 lift)	SPWEA440E	2017-168	Lift 1	1.5
995				UTBWC	2017-146	Lift 1	0.75

There are multiple motivations encompassed in the fulfillment of Task-2. First, to summarize the extensive amount of lab performance testing, field performance data and NRRA member survey results to develop a database of asphalt overlay performance. Results from lab performance tests in combination with cost and performance data available from pavement management systems of NRRA agencies will ultimately be used to assess life cycle performance of MnROAD test sections. Secondly, since the number of variables that can be assessed in test sections is limited due to time and cost constraints, pavement performance modeling will be undertaken in Task-3. The extensive amount of lab performance testing on material characterization will be instrumental in determining model input parameters. Models calibrated and validated with field performance data from test sections will then be used to performed parametric evaluations to have a sufficiently large enough database for development of a simple decision tree tool to select asphalt overlays on PCC pavements.

2. Summary of Laboratory Tests, Results and Discussion

2.1. Disk-Shaped Compact Tension (DCT)

Disk-shaped compact tension (DCT) testing was performed following MnDOT modified procedure for ASTM D7313. Testing was conducted by the MnDOT Office of Materials and Road Research for the 8 study mixtures with 12 replicates and the average fracture energy and fracture strain tolerance was determined for each. In addition to evaluating mixture crack resistance performance using both fracture energy and fracture strain tolerance, comparisons can be made to field performance data and assess the variability of both index parameters.

Fracture Energy (G_f)

Average Fracture energy results for the 8 mixtures are shown in Figure 1, where error bars represent one standard deviation. All mixtures are above the required threshold of 400 J/m^2 as denoted by the solid red line. SPWED430I mixture had the highest G_f with a value of 572 J/m^2 while SPWEB340C mixture had the lowest value of G_f at 447 J/m^2.

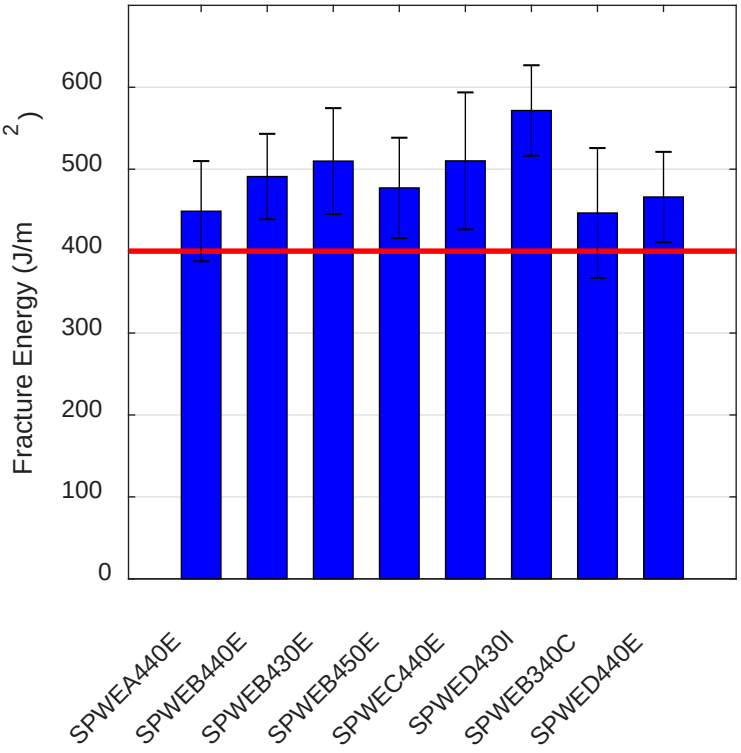

Figure 1: Fracture energy results from DCT testing.

Fracture Strain Tolerance (FST)

Fracture strain tolerance (FST) is an another common index parameter that can be determined from DCT testing (Yue et al. 2018). FST normalizes fracture energy (G_f) by fracture strength (S_f) as shown in Equation 1.

$$FST = \frac{G_f}{S_f} \quad \text{Eqn. 1}$$

S_f is defined in Equation 2, where (P_{max}) represents the maximum load, (w) is the specimen width, and (a) is the ligament length.

$$S_f = \frac{2P_{max}(2w+a)}{b(w-a)^2} \quad \text{Eqn. 2}$$

Figure 2 summarizes the average FST results for all 8 mixtures. Error bars represent one standard deviation. The mixtures all yielded comparable ranking where the mixture with highest FST value was SPWEB430E at a value of 7.17×10^{-6} m and the lowest mixture was SPWEA440E with a value of 6.15×10^{-6} m.

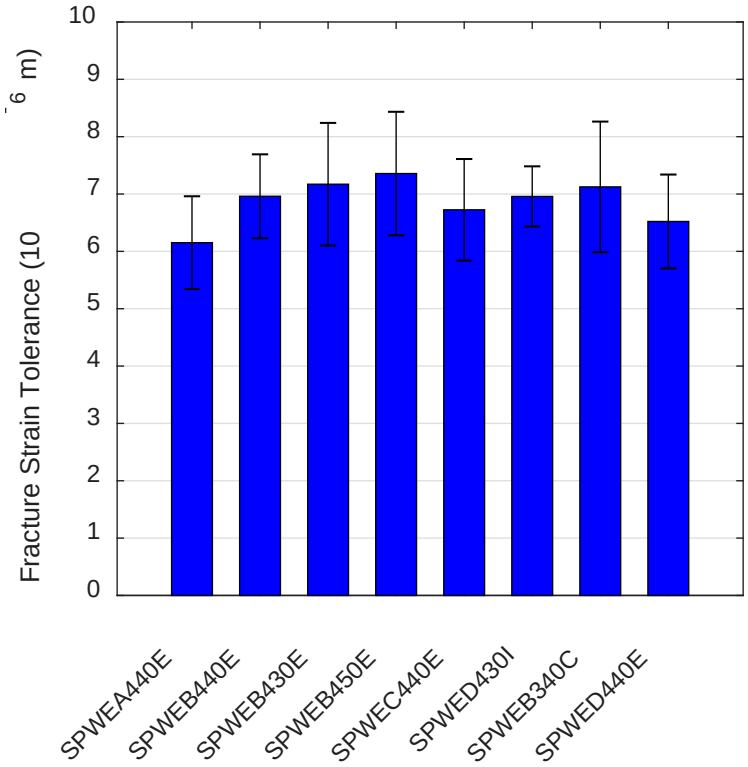

Figure 2: Fracture strain tolerance results from DCT testing.

2.2. Illinois Flexibility Index Semi-Circular Bend Test (I-FIT)

Semi-circular bend testing was conducted following AASHTO TP 124 by IDOT. From this test, the Illinois flexibility index, cracking rate index (CRI) and a rate dependent cracking performance index (RDCI) were calculated.

Flexibility Index (FI)

The flexibility index (FI) was developed to correlate the crack growth velocity and the brittleness of a given mixture. Higher FI values are desirable for asphalt mixtures, as it may indicate better crack resistant mixtures. FI is calculated using Equation 3, where (A) is a unit correction coefficient taken as 0.01, G_f is fracture energy (J/m^2) and m is the slope at the post-peak inflection point.

$$FI = A * \frac{G_f}{abs(m)}$$ Eqn. 3

Figure 3 shows that all mixtures had a relatively high FI average value, exceeding the recommend threshold value of 8. Once again, error bars represent one standard deviation. It is not surprising that SPWED430I had the highest FI value (26.4), since it is a NMAS 4.75 mm mixture with 8.2% asphalt content and designed to be stress absorbing interlayer mixture.

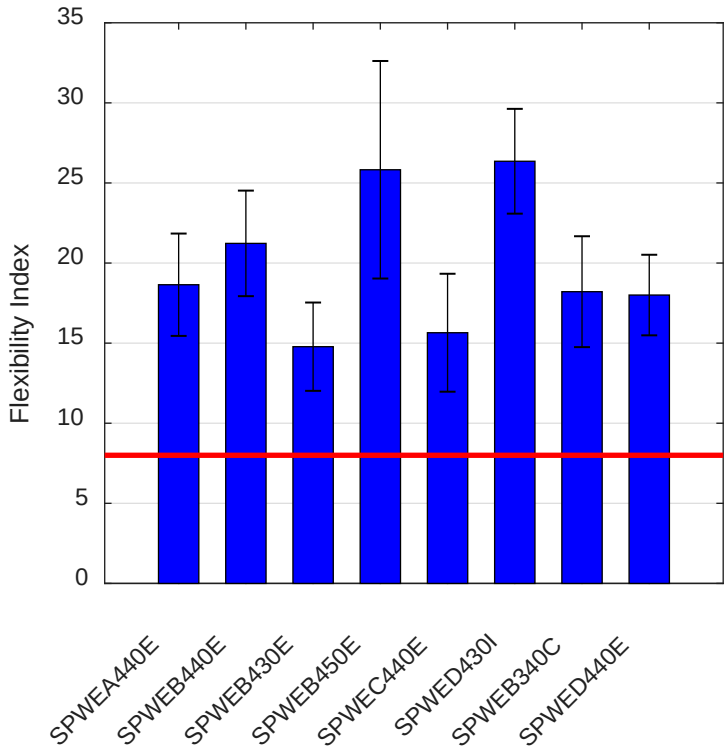

Figure 3: Flexibility index from SCB testing.

Cracking Rate Index (CRI)

Another common performance index used to distinguish cracking resistance is the cracking rate index (CRI) developed by Kaseer et al., 2018. A higher CRI value is desirable for better crack resistance performance. Rather than using the slope at the post-peak inflection point, the peak load (P_{max}) is used to normalize G_f. CRI can be calculated using Equation 4.

$$CRI = \frac{G_f}{abs(P_{max})}$$ Eqn. 4

Figure 4 presents the average CRI results with error bars representing one standard deviation. In general, CRI results agree with the ranking of mixtures using FI. The one exception is for the SPWEB340C and SPWED440E mixtures where a switch in ranking occurred. However, the switch in rank is within the standard deviation of the tested specimens.

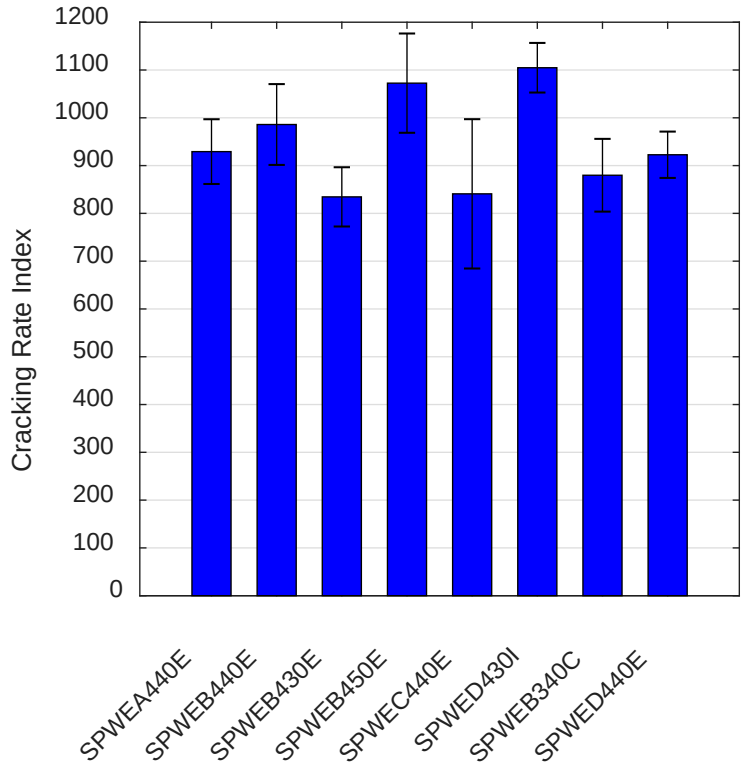

Figure 4: CRI results from SCB testing.

Rate-Dependent Cracking Index (RDCI)

A relatively new rate-dependent cracking index was proposed by Nemati et al. (2019), which utilizes cumulative fracture work potential and instantaneous power calculated from I-FIT results to assess the impulse of the mixture. Similar to FI which evaluates the fracture energy and crack velocity, RDCI follows similar process but does so in a rate-dependent manner. By using the cumulative work over time it exhibits the history of the dissipated work during the crack growth phase and can be used to indicate the crack resistance rate at any time during the loading period. The rate of work over time ($\Delta W/\Delta t$) is defined as power (P). Considering a small range of time, such that when Δt approaches 0, it can be reasonably assumed that power is the rate of the work with respect to time (i.e $\Delta W/\Delta t \approx dW/dt$). Typically, this slope is referred to as the instantaneous power (P_t), which can be considered a scalar quantity indicating the instantaneous energy dissipation rate as shown in Equation 5 and simplified to Equation 6.

$$P_t = \frac{dW}{dt} = \boldsymbol{F}\frac{dx}{dt}; \frac{dx}{dt} = \boldsymbol{V} \qquad \text{Eqn. 5}$$

$$P_t = \boldsymbol{F} \cdot \boldsymbol{V} \qquad \text{Eqn. 6}$$

Equation 7 can be used to calculate RDCI where $\int_{t_{peak}}^{t_{0.1peak}} W_c \ .dt$ is the post peak area under the cumulative work vs time curve (Figure 5), P_{tpeak} is the instantaneous power at peak force, C is a unit correction factor set to 0.01, and the ligament area is the product of specimen thickness and ligament length.

$$RDCI = \frac{\int_{t_{peak}}^{t_{0.1peak}} W_c \ .dt}{P_{tpeak} \times ligament\ area} \times C \qquad \text{Eqn. 7}$$

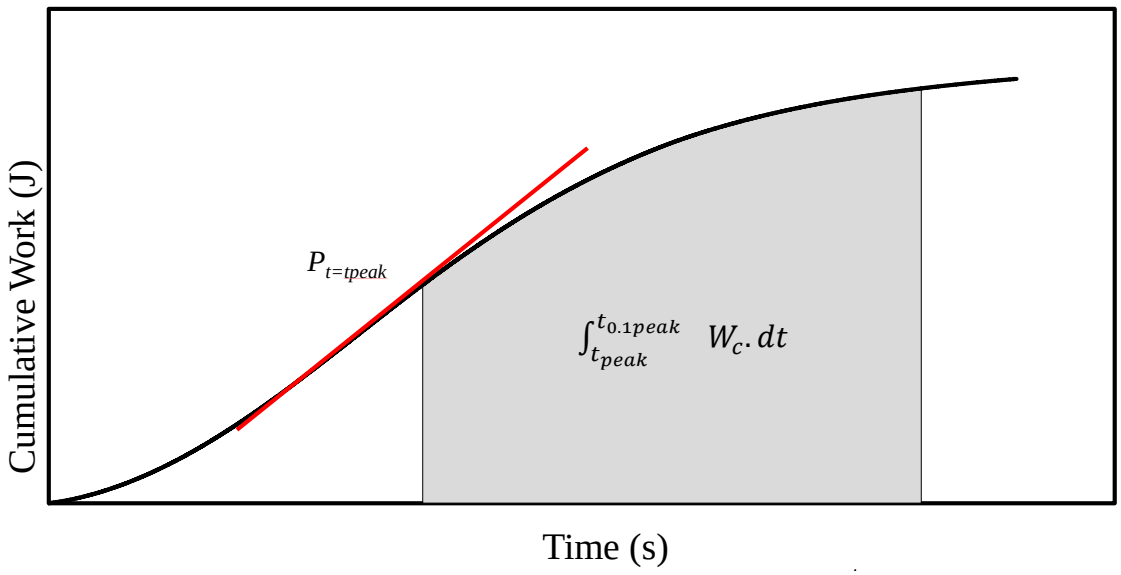

Figure 5: Example of the determination of cumulative work between time at peak load and 0.1 of peak load.

Figure 6 summarizes the average RDCI results with one standard deviation error bars. Overall the ranking of mixtures for RDCI is consistent with that of FI.

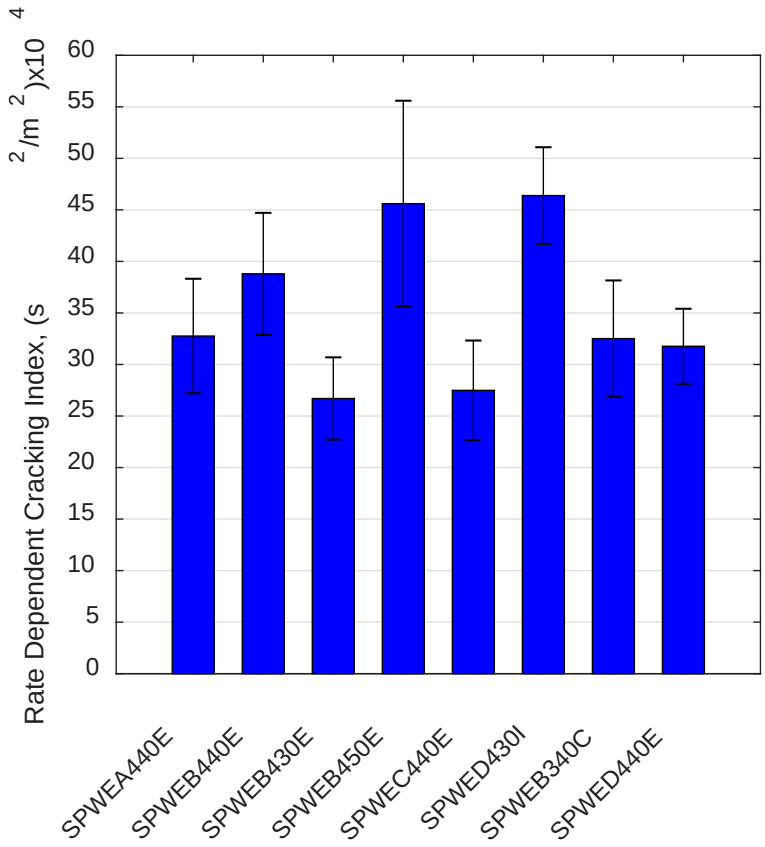

Figure 6: RDCI results from SCB testing.

2.3. Complex (Dynamic) Modulus (E*)

The complex modulus test was performed in accordance with the AASHTO TP342 standard. The dynamic modulus master-curve provides useful information regarding the relative stiffness and rutting susceptibility of one mixture compared to another. It is important to note that all samples are tested at 7% target air void per AASHTO T342 standards.

Dynamic modulus testing results in Figure 7, show that as the design air void level increases from 3% to 5%, stiffness decreases (SPWEB430E > SPWEB440E > SPWEB450E). SPWED440E mixture had the exhibited the lowest overall stiffness behavior, denoted by the green star marker. In general, both NMAS 4.75 mm mixtures had lower stiffness compared to mixtures with NMAS of 9.5 mm, 12.5 mm and 19 mm.

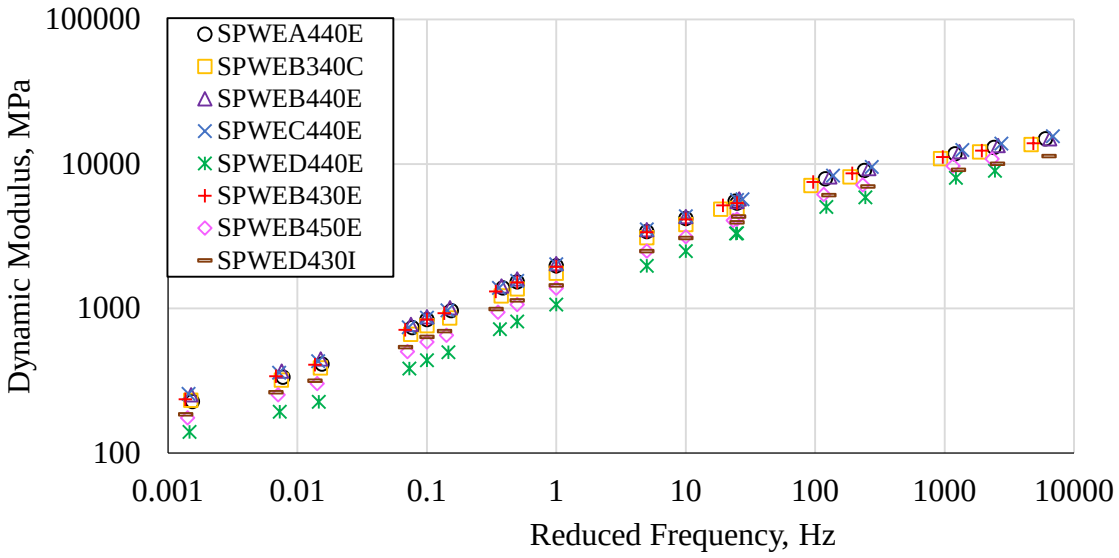

Figure 7: Dynamic modulus master curve at a reference temperature of 21.1◦C.

Phase Angle

The phase angle master curve provides insight on the relative proportion of viscous and elastic behavior of the 8 mixtures at a given temperature and frequency. In general, a higher phase angle means more viscous behavior corresponding to better cracking performance, while lower phase angle (more elastic behavior) may indicate cracking susceptibility. The phase angle for all mixtures is shown in Figure 8. For the 4.75 mm mixtures, SPWED440E had the highest phase angle compared to SPWED430I. Comparisons among the 12.5 mm mixtures show that the SPWEB450E mixture had the highest phase angle while SPWEB340C had the lowest phase angle.

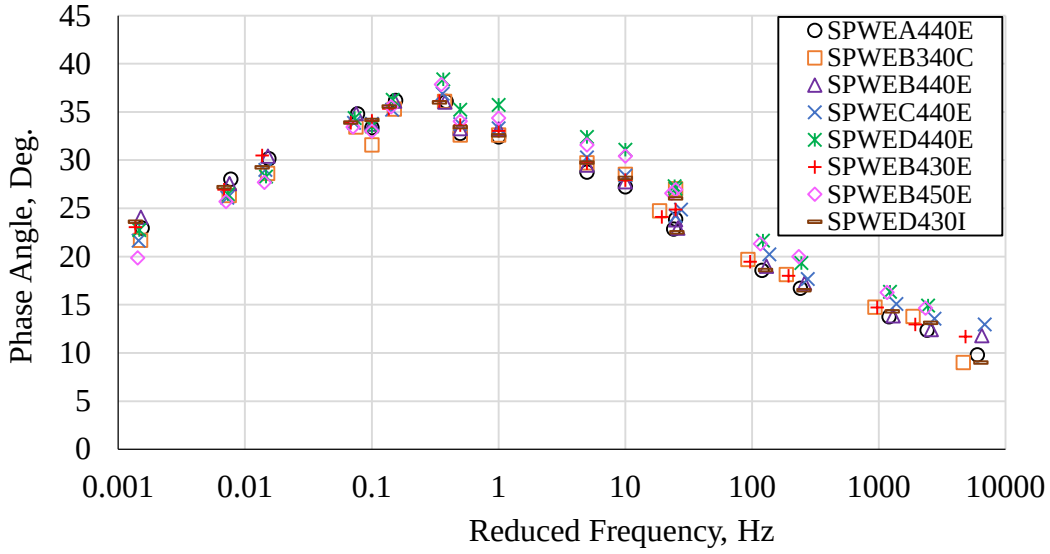

Figure 8: Phase angle master curve.

Black Space

Black space, which cross plots dynamic modulus with phase angle, provides another means of visualizing the rheological behavior of a given mixture while eliminating frequency. Mixture cracking resistance is affected by both stiffness and relaxation capabilities as indicated by dynamic modulus and phase angle respectively. Therefore, mixtures which exhibit higher relaxation capability (higher phase angle) with lower stiffness may result in better cracking resistance behavior. Trends in mixture performance in black space (Figure 9) are consistent with dynamic modulus and phase angle master curves. For example, interlayer mixture SPWED440E which has a NMAS of 4.75 mm, exhibits higher phase angle while maintaining relatively lower stiffness compared to other mixtures.

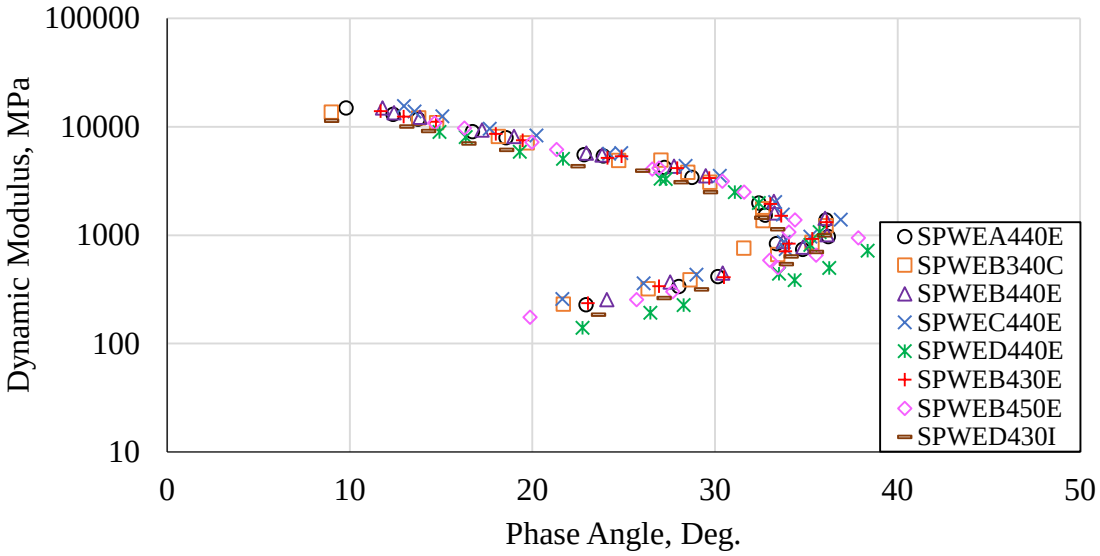

Figure 9: Black space diagram.

2.4. Overlay Tester (OT)

The Texas overlay tester (OT) has been proposed as a test method to determine the susceptibility of HMA mixtures to fatigue or reflective cracking. In this study, OT was performed by IDOT following the TX-248-F procedure. There are several different ways to analyze OT results, some of which include load reduction as function of load cycles applied, load reduction at 1000 cycles, and the number of cycles it takes to achieve 93% load reduction (failure). In terms of cracking performance, the higher the number of cycles to achieve failure the better expected crack resistance. When comparing load reduction at 1000 cycles (single point), lower load reduction is preferred for better crack resistance performance.

Load Reduction

Figure 10 shows load reduction as a percentage with respect to the number of loading cycles applied for all 8 mixtures. For each mixture, 5 replicates were tested and averaged. It can be observed from this plot that SPWED430I has the lowest load reduction (better performance), while SPWEB440E has the highest load reduction after only approximately 1600 cycles.

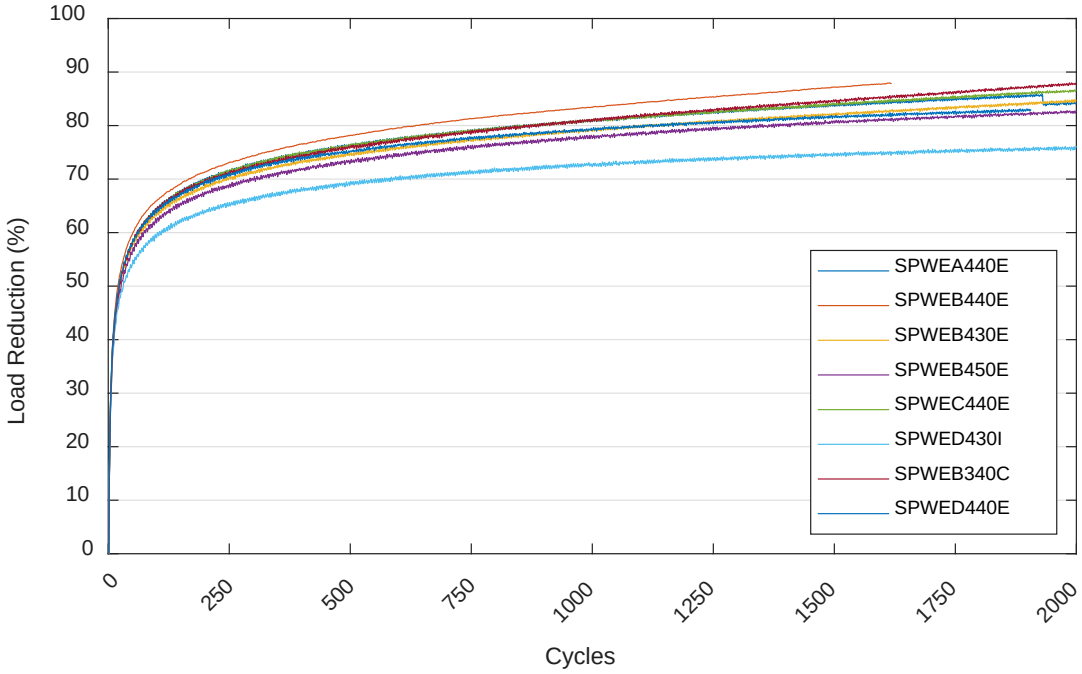

Figure 10: Load reduction for all mixtures from overlay tester.

Percent load reduction at 1000 cycles from Figure 10 was selected as a comparison point among the 8 mixtures and is shown in Figure 11. Results at the single point comparison point agrees with the general trend in ranking of mixtures with SPWED430I still as the best performer and SPWEB440E as the worst performer.

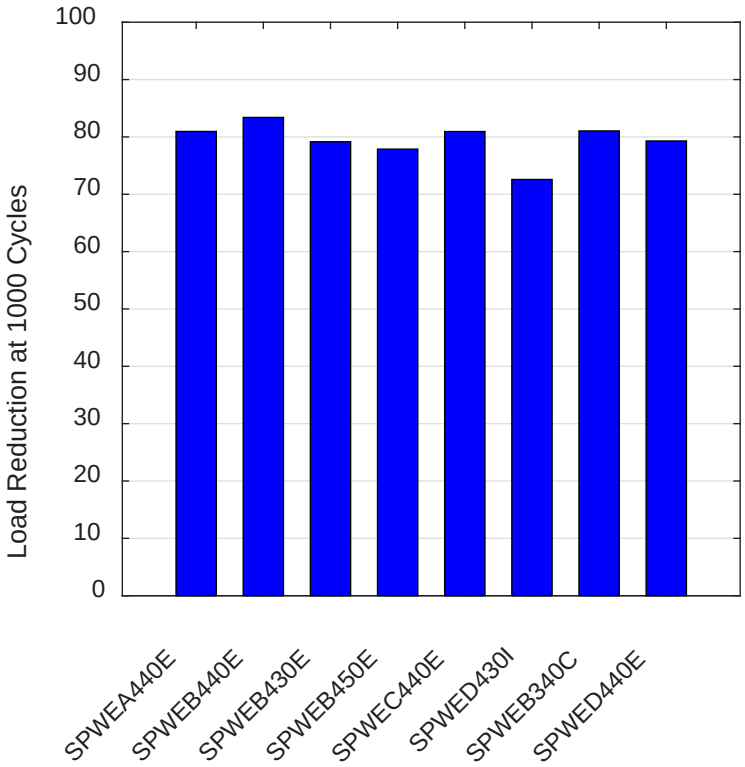

Figure 11:Overlay tester results at 1000 cycles.

Cycles to Failure

The number of cycles at 93% load reduction (test failure point), is represented in Figure 12. It is more evident in this plot that from laboratory testing, SPWED430I is expected to have better resistance to fatigue or reflective cracking. Results from other mixtures were relatively comparable with SPWEB440E having the lowest number of cycles to achieve 93% load reduction.

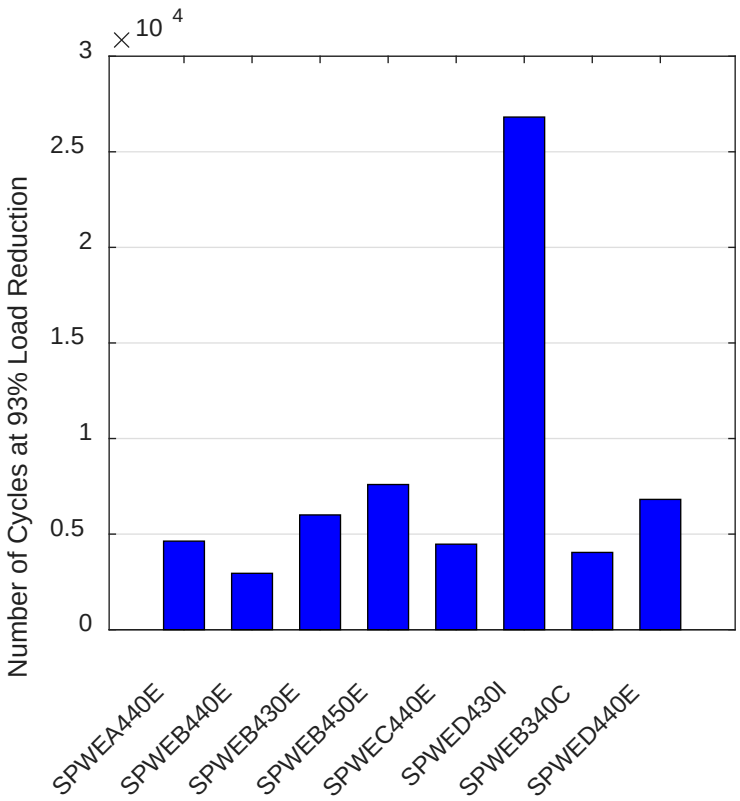

Figure 12: Overlay tester results at 93% load reduction.

2.5. Hamburg Wheel Tracker (HWT)

Hamburg wheel tracker (HWT) test was performed in accordance with AASHTO T-324. This test has gained popularity not only as a rutting performance test but also as a test to evaluate moisture susceptibility. The two most common parameters that are measured from Hamburg results are the stripping inflection point and the final rut depth (typically after 20,000 passes).

The stripping inflection point (SIP) is the location on a typical rut depth versus number of wheel passes plot where the rate of rut depth accumulation (slope) increases significantly. SIP is what allows for the comparison of moisture susceptibility among the different mixtures as damage after the SIP is attributed to the presence of moisture. The SIP is calculated by first identifying the stripping slope and creep slope lines. The SIP is then determined by finding the number of passes at which the creep slope and stripping slope lines intersect.

Each mixture was tested under a right and left wheel path in the Hamburg wheel tracking device to provide two replicates for each mixture. Figure 13, summarizes the SIP results for all mixtures. In general, the SIP is used as a pass or fail parameter by many states with a typical threshold value of 10,000 passes. Only one mixture (SPWED440E) did not meet this recommended threshold value.

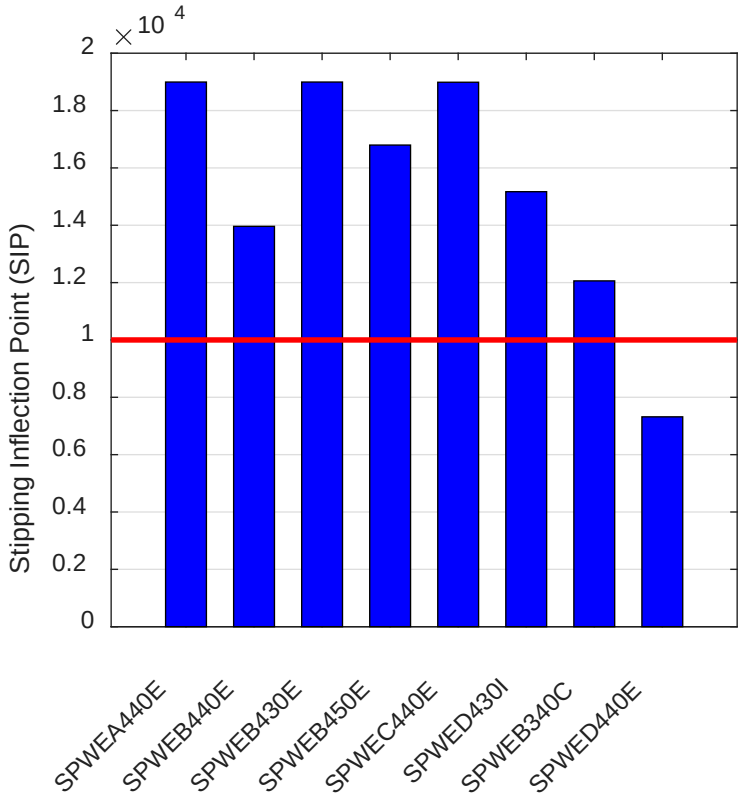

Figure 13: Stripping inflection point for all mixtures.

Figure 14 summarizes the final rut depth using the average of the middle 7 data points for all mixtures after 20,000 passes. Asphalt mixtures with lower rut depth are desirable, and in combination with higher SIP results may indicate mixtures that are more resistant to moisture-induced damage compared to those mixtures with lower values.

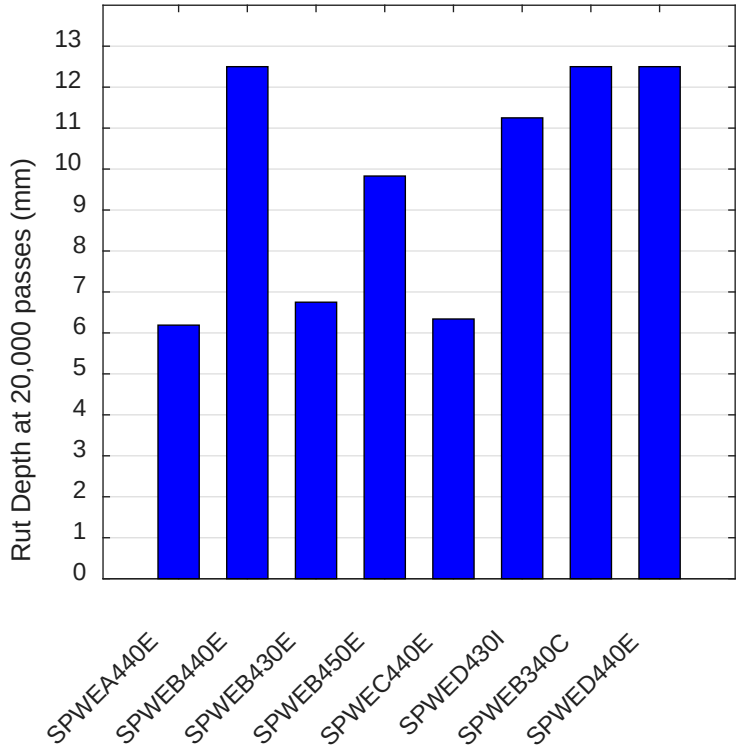

Figure 14: Rut depth results at 20,000 passes for all mixtures.

A relatively new method to analyze HWT results was proposed by Yin et al. (2014) (TTI method) and aims to analyze the rutting and stripping damage of the Hamburg curve separately. The motivation behind developing this analysis method is to reduce the variance in determining the SIP. Following the AASHTO T-324 standard procedure to determine the SIP can be influenced significantly by the algorithms used to find the creep slope and tripping slope lines. A slight deviation in either of these lines will impact the calculated SIP value and in turn affect the conclusions drawn about a given material's moisture susceptibility. Therefore, in this study the TTI method was also used to evaluate mixtures moisture susceptibility.

There are two parameters of interest to evaluate moisture susceptibility from Hamburg results using the TTI method, stripping number (LC_{SN}) and stripping life (LC_{ST}). First the raw Hamburg data is fit using Equation 8 where RD is rut depth, LC is load cycles and B, p, LC_{ult} are fitting coefficients.

$$RD = p * \left[\ln\left(\frac{LC_{ult}}{LC}\right)\right]^{\frac{-1}{B}} \quad \text{Eqn. 8}$$

Once fitted, the point where the number of load cycles at which the accumulated rut depth begins to increase again after the creep phase of the test is determined by setting the second derivative from Equation 8 equal to 0. To directly solve for the stripping number Equation 9 can be used where B and LC_{ult} are fitting coefficients from Equation 8.

$$LC_{SN} = LC_{ult} * \exp\left(-\frac{B+1}{B}\right) \quad \text{Eqn. 9}$$

The second parameter of interest using the TTI method is the stripping life (LC_{ST}). To calculate LC_{ST}, first the accumulated rut depth is zeroed at the LC_{SN} point. Equation 10 is then used to fit the data points after the LC_{SN} point where ε^{st} is the stripping strain, ε_0^{st} is the initial stripping strain, LC represents load cycles and θ is a fitting coefficient.

$$\varepsilon^{st} = \varepsilon_0^{st} * (e^{\theta(LC - Lc_{SN})} - 1) \quad \text{Eqn. 10}$$

Once Equation 10 is fit, then LC_{ST} is calculated by determining the number of load cycles after the stripping number that is required to induce 0.2 stripping strain in the material. A value of 0.2 is proposed in the TTI method to correspond to 12.5 mm of deformation on a standard 62.5 mm height specimen. Equation 11 can be used to solve directly for LC_{ST}.

$$LC_{ST} = \frac{1}{\theta} * \ln(\frac{12.5}{T * \varepsilon_0^{st}} + 1) \quad \text{Eqn. 11}$$

It should be noted that for mixtures where there is no inflection point, stripping number and stripping life cannot be determined. An example of a mixture where no inflection point exists is included in the Appendix.

In summary, the stripping number captures how many load cycles are required before moisture begins to break down the bonds between aggregates and mastic. All rut depth accumulation before this point can be attributed to visco-plastic effects, while all additional rut depth after this primarily due to stripping damage. Stripping life describes how quickly the stripping damage evolves after its initial onset. A higher stripping number and stripping life value is desirable. Results of stripping number and stripping life are presented in Figure 15 and Figure 16 respectively.

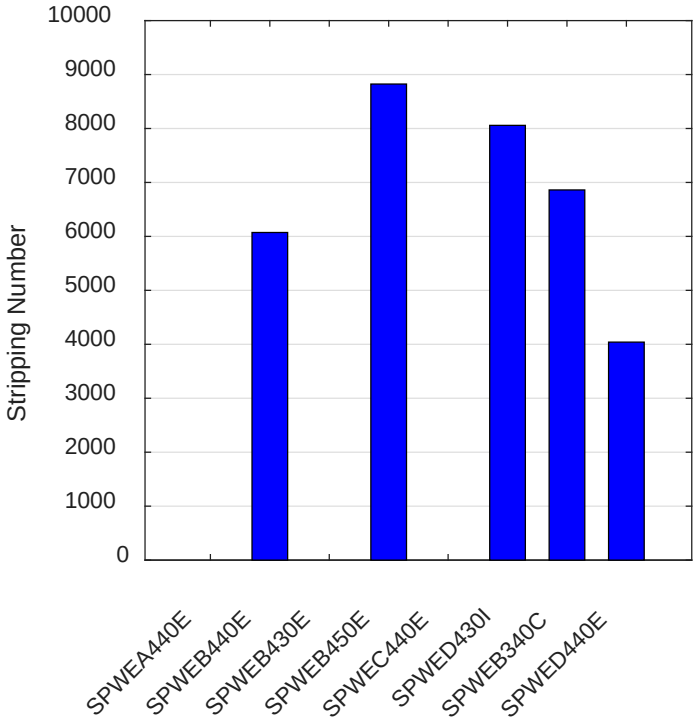

Figure 15: Stripping number results using TTI method.

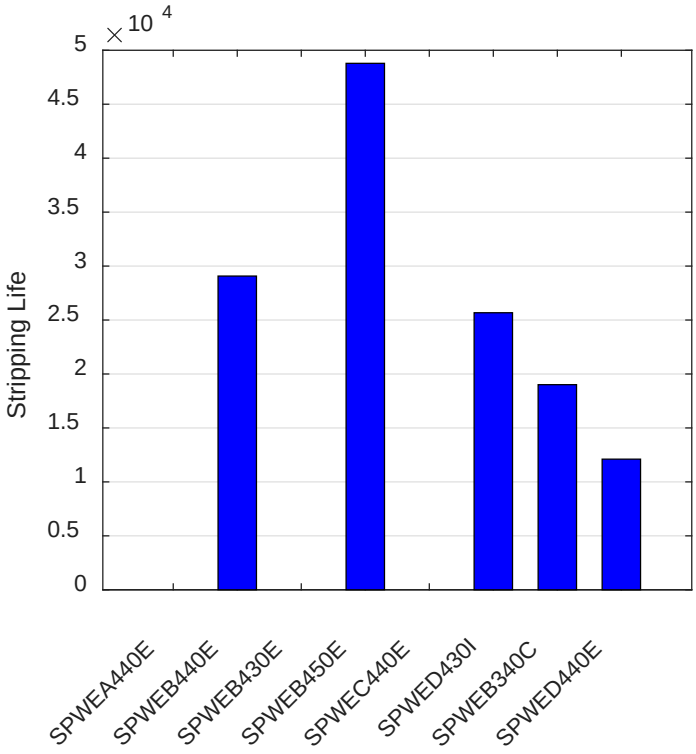

Figure 16: Stripping life results using TTI method.

2.6. Tensile Strength ratio (TSR)

Tensile strength ratio (TSR) testing was performed following two different conditions methods, AASHTO T-283 and moisture induced stress tester (MiST) conditioning. MODOT was responsible for performing testing per AASHTO T-283 specifications. Tensile strength ratio values for all mixtures as a percentage is shown in Figure 17, while tensile strength is shown in Figure 18. Table 4 summarizes the TSR results provided by MODOT.

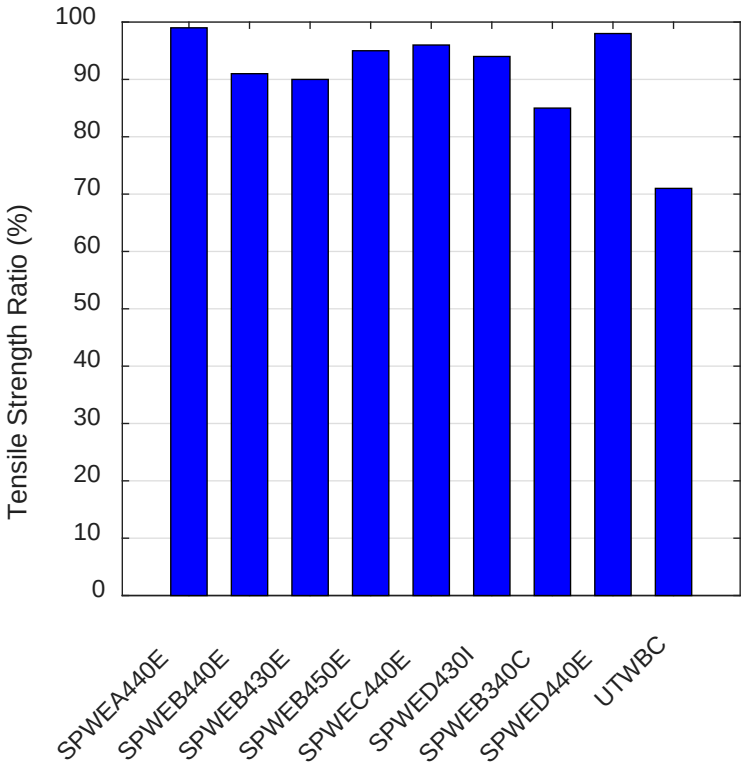

Figure 17: AASHTO T- 283 tensile strength results from MODOT.

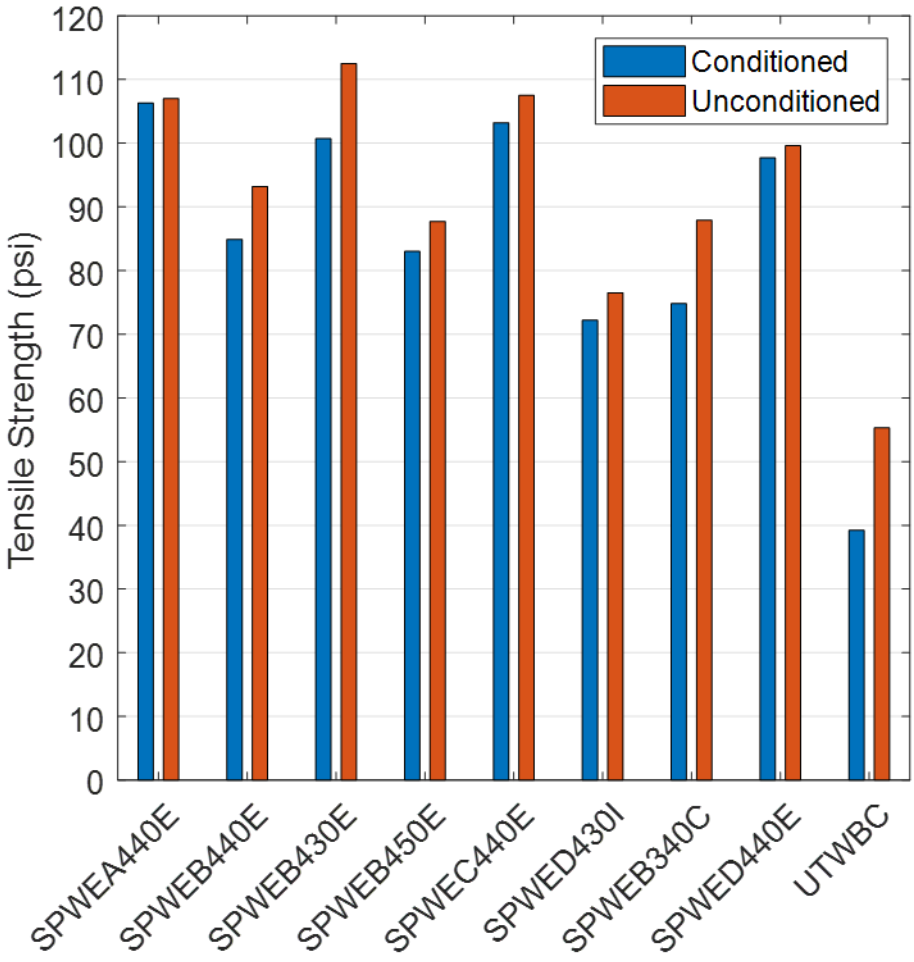

Figure 18: Tensile strength results from MODOT.

Table 4: Summary of tensile strength ratio data from MODOT.

Mixture	Average Gyrations	Tensile Strength Average (psi)		Average Air Voids		Average Saturation (%)	TSR (%)
		Conditioned	Unconditioned	Wet Set	Dry Set		
SPWEA440E	26	106.3	107	6.8	6.8	75	99
SPWEB440E	20	84.9	93.2	7.1	7.2	80	91
SPWEB430E	34	100.7	112.5	7.1	7.1	78	90
SPWEB450E	16	83	87.7	6.9	7	78	95
SPWEC440E	33	103.2	107.5	7	7.2	78	96
SPWED430I	12	72.2	76.5	6.8	7	79	94
SPWEB340C	25	74.8	87.9	7.2	7.4	77	85
SPWED440E	25	97.7	99.6	6.8	6.9	80	98
UTBWC	50	39.2	55.3	10.8	10.9	72	71

MTU performed MiST condition on specimens for 500 cycles and 3500 cycles and the TSR results are shown in Figure 19. A typical TSR threshold value of 0.8 was used to distinguish good and poor performance among the mixtures. All mixtures met the threshold value except for SPWEB340C mixture after undergoing 3500 cycles of conditioning and SPWEB440E after 500 cycles of conditioning.

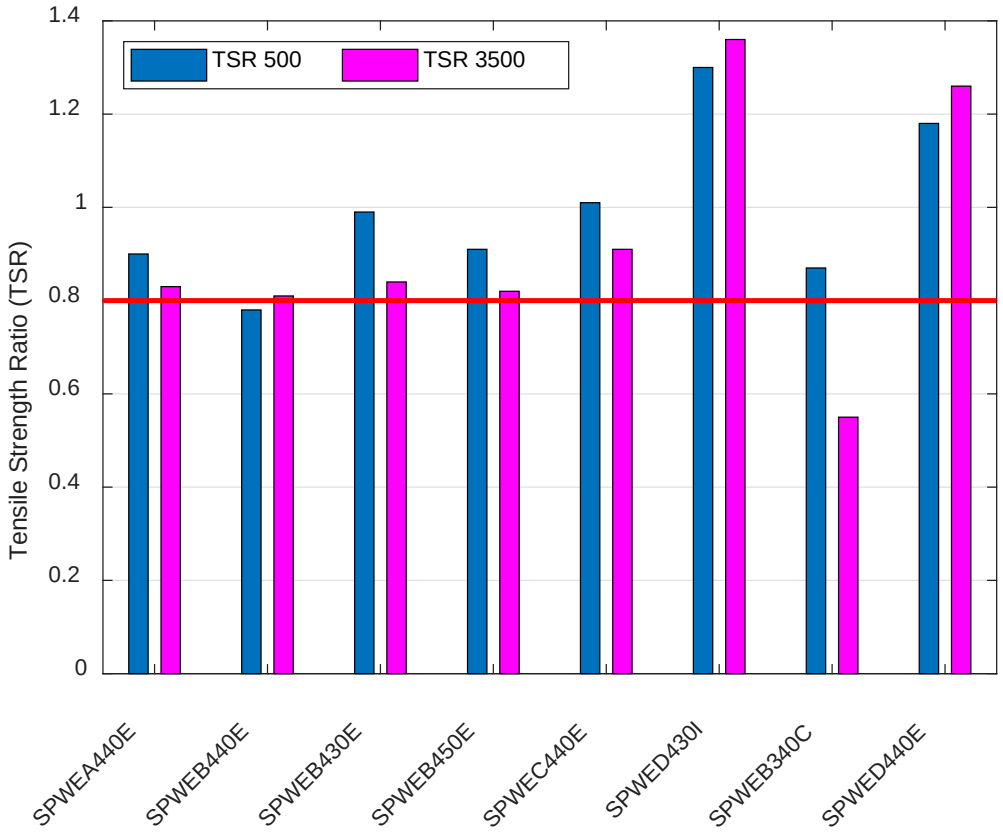

Figure 19: TSR results at 500 cycles and 3500 cycles of MIST conditioning from MTU.

Average indirect tensile strength values from three replicates of dry and conditioned specimens after 500 and 3500 cycles is reported in Figure 20. In general, it is expected that dry specimens would have the highest IDT value followed by specimens conditioned at 500 cycles and then 3500 cycles. This trend is observed in all mixtures except for SPWED430I and SPWED440E. It was noted by MnDOT researchers that these two mixtures may have segregation issues. Also, the average air void level for these two mixtures was lower than the recommended 7.0 % ± 0.5, which may contribute to the reverse trend in expect IDT performance ranking.

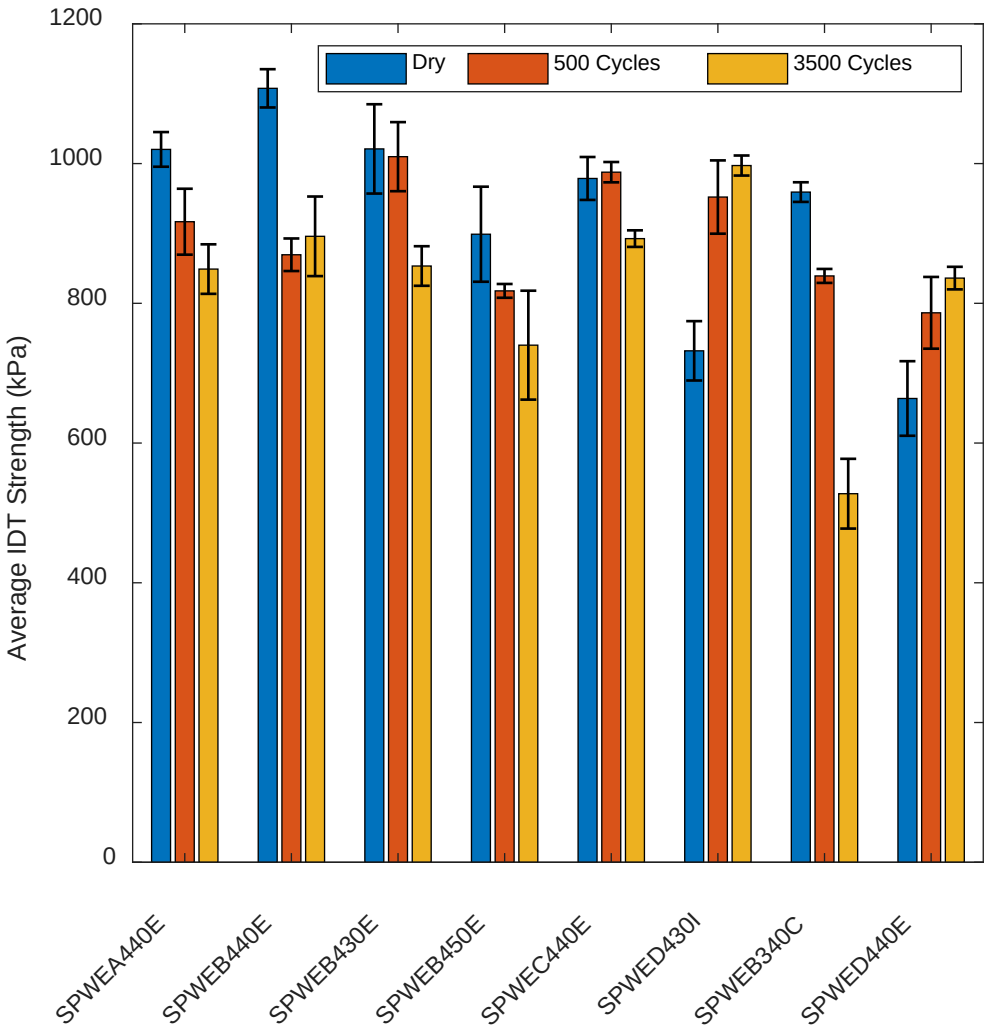

Figure 20: Average IDT strength comparison of dry and conditions specimens.

3. Summary of Field Performance Data

3.1 Joint Opening Data

Joint opening (JO) data was provided for four test sections (983, 984, 989 and 992) for approximately one-year duration (September 2017 to 2018). A new type of linear potentiometer sensing system developed by MnROAD researchers was used to measure the change in transverse joint opening due to changing environmental conditions. Figure 21 provides an example of the JO sensor set up between PCC concrete panels.

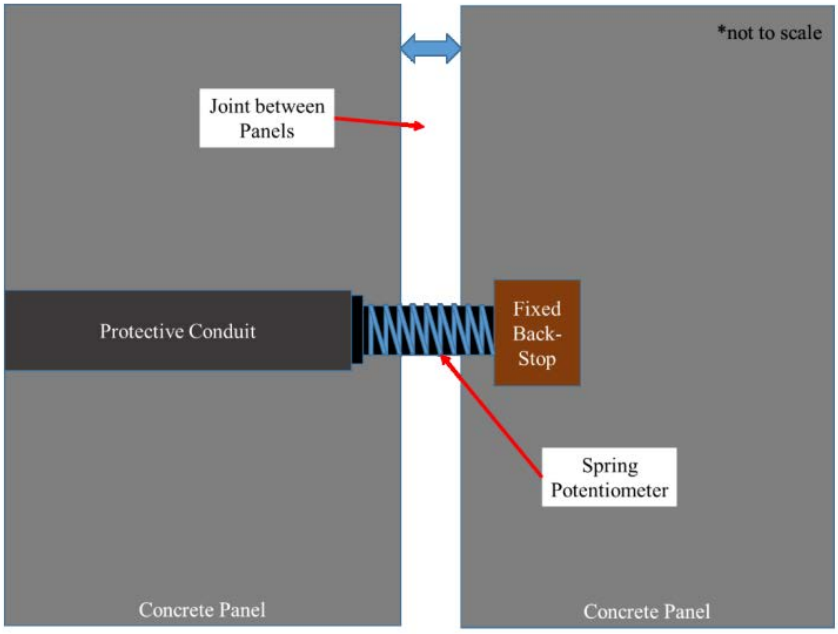

Figure 21: Schematic diagram of joint opening (JO) sensor in underlying PCC panels (Van Deusen et al., 2018).

Joint movement is determined using a spring potentiometer, which is inserted into a conduit on one side of the joint and connects with an angle-iron bracket mounted on an adjacent concrete panel as shown in Figure 21. As panels expand and contract due to changes in temperature, it causes the sensor inside the piston to compresses and expands accordingly. This expansion and contraction results in a change in resistance, where 0 mV corresponds to full extension and approximately 5000 mV to full compression. There are two JO sensors located in cell 983, while cells 984, 989 and 992 contain three JO sensors. Data is recorded on 15 minute increments. Figure 22 provides time history of the movement at joint locations within each respective test section.

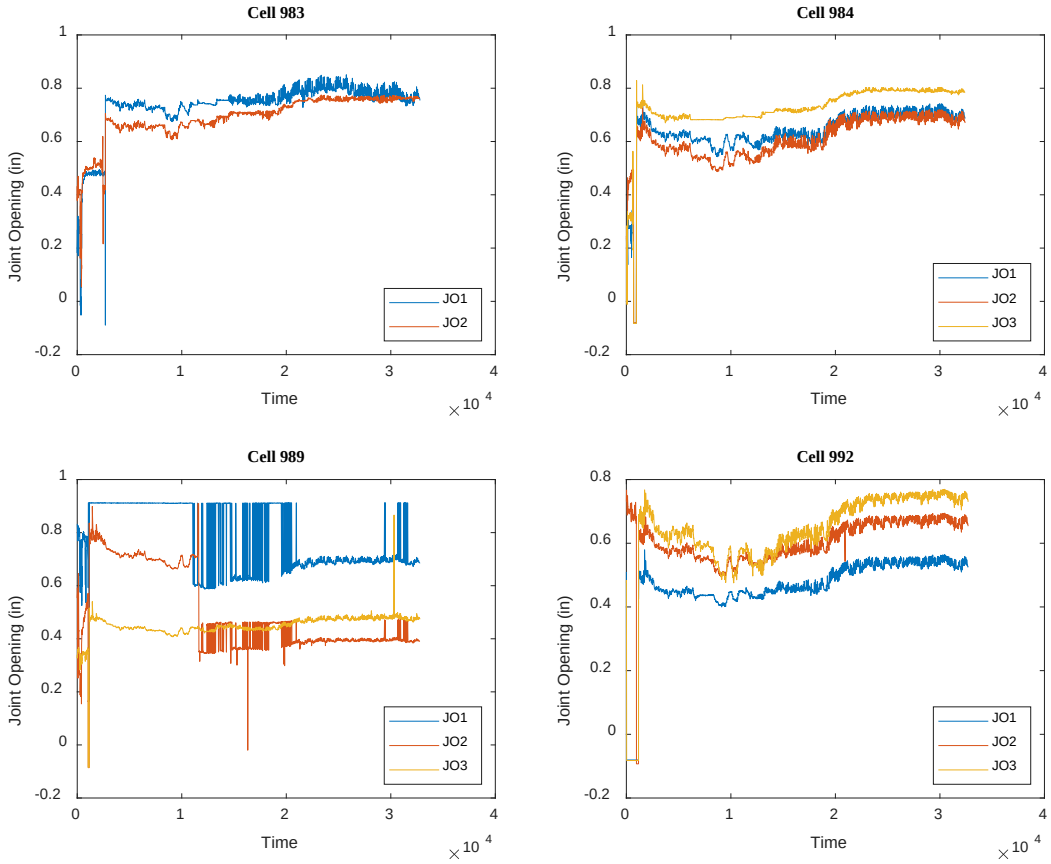

Figure 22: Joint opening data for test sections 983, 984, 989 and 992.

3.2 Crack Distress Maps

Condition survey results were performed by MnDOT in May and November of 2018. Figure 23 shows an example of a distress map for test cell section 994.

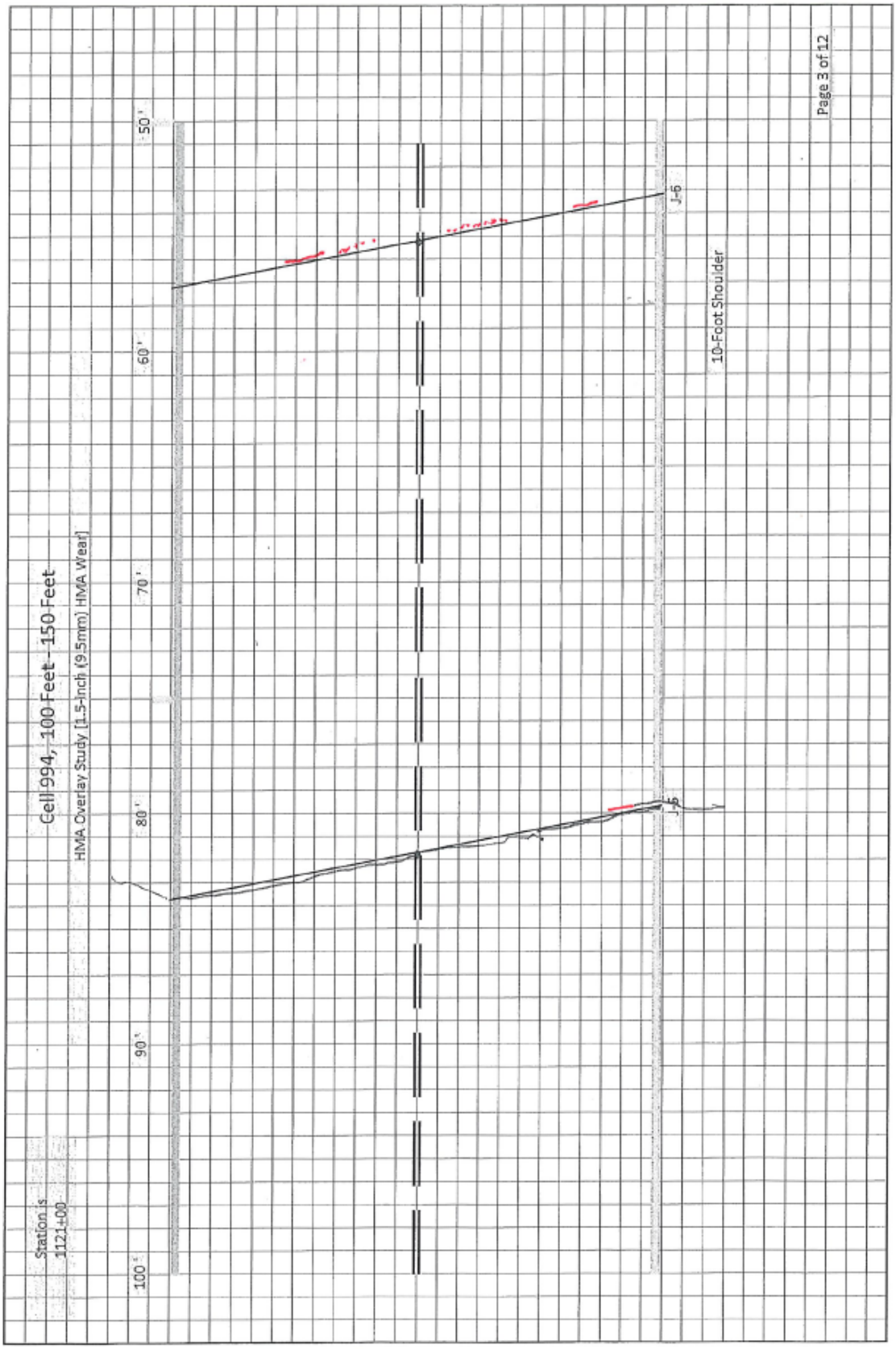

Figure 23: Example of distress crack map for cell 994.

Crack distress maps were converted into a percentage of joints cracked within each test section excluding the transition zones. This was accomplished by first taking an inventory of all crack maps and quantifying the crack length at each joint on a scale from 0 to 1, where 0 represents no crack at the joint and 1 represents a joint that is fully cracked along the lane width. The percent of joints cracked within a test cell was calculated by taking the sum of crack lengths at each joint and normalizing by the total number of joints within the test cell section. Figure 24 provides an example of the percentage of joints cracked as of November 18th, 2018 for test sections 984-994. Information for the UTBWC test section (cell 995) was not provided to researchers, therefore not included in the comparison of field cracking performance.

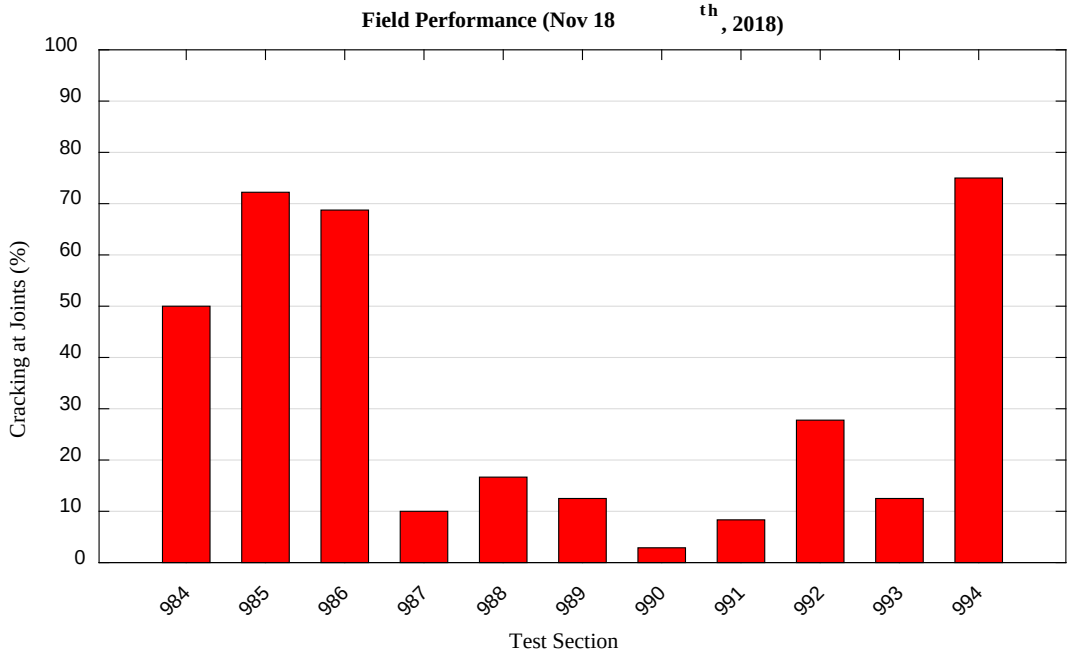

Figure 24: Summary of cracking located at joints as of Nov 18th, 2018.

After just one year of placement, test sections with less than 10% cracking at joints include cell 990 (1.5", 9.5 mm (3% AV) and 2.25" HMA, 19mm), cell 991 (1.75", 9.5mm (AASHTO M323 #8) and 2.25" HMA, 19mm) and cell 987 (1.5" HMA, 9.5mm and 2.5" HMA, 19mm). Meanwhile, the test cell section 994 had the highest amount of cracking located at the joins (75%).

3.3 Overlay Load Transfer Efficiency (LTE)

Falling weight deflectometer (FWD) testing is a valuable test method to evaluate physical properties of asphalt overlays. Prior to overlay construction FWD testing can be used to determine the structural capacity of the existing PCC, while after overlay construction FWD can be used to determine if the overlay structure is being overloaded. FWD was performed prior to overlay construction (June 2017) to assess structural capacity of the existing PCC on test cell sections 984 to 995. Data was recorded on April 5th, 2017 for the driving and passing lanes respectively and is shown in Figure 25.

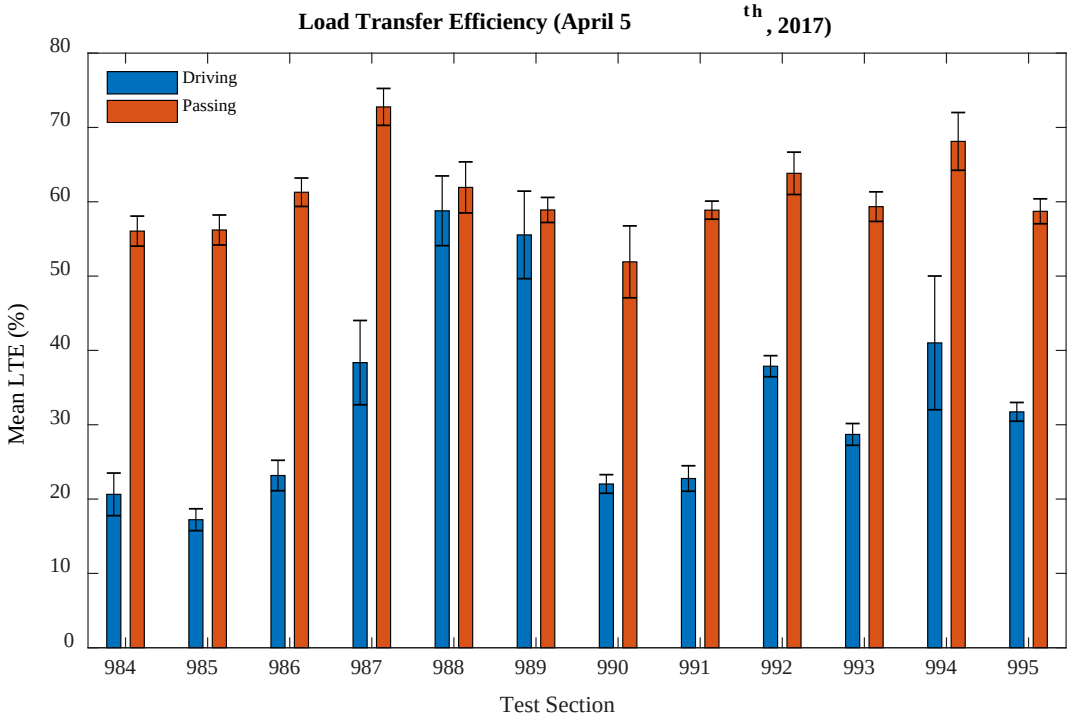

Figure 25: Load transfer efficiency data on test sections 984-995.

Table 5 summarizes statistical analysis performed on the FWD results prior to overlay construction. Included in Table 5 is the mean LTE, standard error, median standard deviation, sample variance, kurtosis, skewness, range, minimum and maximum LTE for each test section in the driving and passing lanes respectively. This basic statistical information provides insight into the variability of the collected LTE data. Skewness described the dataset's symmetry or lack of symmetry where a normal distribution has a skewness of 0. Meanwhile, kurtosis results provide a measurement of the combined sizes of the two tails from a given dataset. Range of the data set is simply the difference between the largest and smallest value. Together, information from Table 5 can be used to assess the variability of the measured data at different points in time. After construction of overlays with varying HMA materials and thicknesses, FWD testing can be performed again to verify the LTE of different sections and draw conclusions on the effectiveness of each test section overlay to distribute load at joints.

Table 5: FWD statistics summary for test sections 984-995.

Cell	Lane	Mean	Standard Error	Median	Standard Deviation	Sample Variance	Kurtosis	Skewness	Range	Minimum	Maximum
984	Driving	20.63	2.87	17.20	8.11	65.75	2.248	1.657	23.63	14.02	37.65
985		17.22	1.47	17.07	4.15	17.26	-1.421	-0.025	11.21	11.92	23.13
986		23.17	2.05	22.89	5.79	33.52	-0.393	0.245	17.78	14.53	32.31
987		38.36	5.67	37.19	18.80	353.61	-1.244	0.236	51.67	14.14	65.81
988		58.78	4.69	59.30	13.27	175.96	-0.472	-0.408	40.34	36.61	76.94
989		55.54	5.89	59.35	18.62	346.69	0.263	-0.891	56.92	22.94	79.86
990		22.03	1.25	21.82	3.31	10.97	2.525	1.294	10.45	18.07	28.52
991		22.77	1.71	22.27	4.84	23.46	0.313	-0.008	15.18	14.59	29.77
992		37.87	1.42	39.00	4.01	16.09	3.154	-1.567	13.16	29.23	42.38
993		28.70	1.47	29.36	4.14	17.17	1.337	-1.165	12.94	20.51	33.45
994		41.01	9.00	29.53	25.45	647.85	-0.043	1.395	60.08	22.92	83.00
995		31.73	1.26	31.14	3.57	12.73	-1.371	0.091	9.85	26.98	36.84
984	Passing	56.05	2.02	55.97	5.71	32.65	-0.267	0.013	17.11	46.79	63.90
985		56.20	2.02	57.11	5.70	32.51	-1.652	-0.090	14.51	48.78	63.30
986		61.28	1.91	61.45	5.40	29.21	-1.378	-0.325	14.12	53.08	67.20
987		72.76	2.48	73.26	7.85	61.63	-1.552	0.078	21.84	62.90	84.74
988		61.93	3.43	60.22	9.71	94.24	-1.799	0.260	25.26	50.09	75.35
989		58.90	1.68	58.06	5.33	28.38	-0.498	0.158	17.17	50.17	67.34
990		51.91	4.84	53.41	13.68	187.24	-0.892	-0.449	38.31	30.18	68.49
991		58.87	1.22	58.65	3.44	11.85	-0.892	0.033	9.76	53.87	63.63
992		63.83	2.85	61.59	8.06	64.95	0.058	0.982	23.18	55.28	78.46
993		59.34	1.99	58.11	5.63	31.69	-0.533	0.837	15.42	52.65	68.07
994		68.12	3.89	64.48	10.99	120.81	-0.439	0.966	30.30	55.96	86.26
995		58.72	1.68	58.44	4.74	22.48	0.705	-0.887	13.90	49.64	63.54

4. Statistical Comparison

4.1 Pearson Correlation

A common statistical method that is used to evaluate the strength of correlation between volumetric and lab mixture performance data is the Pearson correlation. The Pearson correlation is a measure of how much two variables change together. It is typically reported on a scale from 1 to -1 where, 1 represents a strong positive correlation and -1 represents a strong negative correlation. Table 6 summarizes the Pearson correlation for select volumetric properties and performance test results. A color designation was used to identify strong, medium and weak correlation using the following criteria:

- Strong correlation (green): $0.7 \leq |x| \leq 1$
- Medium correlation (orange): $0.3 \leq |x| \leq 0.7$
- Weak correlation (red): $|x| < 0.3$

Table 6: Pearson correlation summary.

Variables	PGLT	UTI	NMAS	AC (%)	Adj. AFT	AV (%)	VMA	RAP	Gyr	% Passing #4	% Passing #200	SA	G_f	FI	CRI	RDCI	IDT (500 cycles)	IDT (3500 cycles)	IDT (Dry)	TSR (500)	TSR (3500)	OT % Load Reduction (2000 cycles)
PGLT	**1.00**	-	-	-	-	-	-	-	-	-	-	-	-	-	-	-	-	-	-	-	-	-
UTI	**-0.34**	**1.00**	-	-	-	-	-	-	-	-	-	-	-	-	-	-	-	-	-	-	-	-
NMAS	**0.17**	**-0.31**	**1.00**	-	-	-	-	-	-	-	-	-	-	-	-	-	-	-	-	-	-	-
AC (%)	**-0.24**	**0.34**	**-0.74**	**1.00**	-	-	-	-	-	-	-	-	-	-	-	-	-	-	-	-	-	-
Adj. AFT	**-0.28**	**-0.07**	**0.43**	**0.21**	**1.00**	-	-	-	-	-	-	-	-	-	-	-	-	-	-	-	-	-
AV (%)	**-0.36**	**-0.46**	**0.38**	**-0.40**	**0.36**	**1.00**	-	-	-	-	-	-	-	-	-	-	-	-	-	-	-	-
VMA	**-0.27**	**0.19**	**-0.83**	**0.85**	**-0.08**	**-0.17**	**1.00**	-	-	-	-	-	-	-	-	-	-	-	-	-	-	-
RAP	**0.38**	**-0.50**	**0.46**	**-0.69**	**-0.12**	**0.28**	**-0.76**	**1.00**	-	-	-	-	-	-	-	-	-	-	-	-	-	-
Gyr	**0.42**	**-0.65**	**0.40**	**-0.63**	**-0.39**	**-0.04**	**-0.53**	**0.56**	**1.00**	-	-	-	-	-	-	-	-	-	-	-	-	-
% Passing #4	**-0.17**	**0.30**	**-0.94**	**0.83**	**-0.35**	**-0.52**	**0.88**	**-0.63**	**-0.32**	**1.00**	-	-	-	-	-	-	-	-	-	-	-	-
% Passing #200	**-0.16**	**0.37**	**-0.89**	**0.82**	**-0.34**	**-0.55**	**0.90**	**-0.74**	**-0.35**	**0.98**	**1.00**	-	-	-	-	-	-	-	-	-	-	-
SA	**-0.10**	**0.30**	**-0.93**	**0.77**	**-0.44**	**-0.57**	**0.86**	**-0.62**	**-0.27**	**0.99**	**0.99**	**1.00**	-	-	-	-	-	-	-	-	-	-
G_f	**0.15**	**0.29**	**-0.14**	**0.60**	**0.27**	**-0.72**	**0.25**	**-0.40**	**-0.20**	**0.37**	**0.42**	**0.38**	**1.00**	-	-	-	-	-	-	-	-	-
FI	**-0.50**	**0.32**	**-0.40**	**0.61**	**0.36**	**0.06**	**0.44**	**-0.22**	**-0.71**	**0.34**	**0.31**	**0.29**	**0.35**	**1.00**	-	-	-	-	-	-	-	-
CRI	**-0.47**	**0.28**	**-0.51**	**0.71**	**0.34**	**0.00**	**0.54**	**-0.26**	**-0.69**	**0.46**	**0.41**	**0.40**	**0.38**	**0.99**	**1.00**	-	-	-	-	-	-	-
RDCI	**-0.48**	**0.34**	**-0.41**	**0.62**	**0.37**	**0.05**	**0.45**	**-0.23**	**-0.74**	**0.34**	**0.31**	**0.29**	**0.35**	**1.00**	**0.99**	**1.00**	-	-	-	-	-	-
IDT (500 cycles)	**0.54**	**-0.01**	**0.36**	**-0.10**	**0.11**	**-0.63**	**-0.48**	**0.25**	**0.42**	**-0.20**	**-0.19**	**-0.18**	**0.59**	**-0.34**	**-0.32**	**-0.34**	**1.00**	-	-	-	-	-
IDT (3500 cycles)	**0.12**	**-0.27**	**-0.23**	**0.48**	**0.08**	**-0.51**	**0.25**	**-0.10**	**0.29**	**0.44**	**0.40**	**0.43**	**0.72**	**0.19**	**0.29**	**0.17**	**0.50**	**1.00**	-	-	-	-
IDT (Dry)	**0.29**	**-0.31**	**0.71**	**-0.84**	**-0.07**	**0.20**	**-0.93**	**0.88**	**0.58**	**-0.80**	**-0.83**	**-0.76**	**-0.26**	**-0.28**	**-0.38**	**-0.30**	**0.35**	**-0.15**	**1.00**	-	-	-
TSR (500)	**-0.05**	**0.33**	**-0.61**	**0.87**	**0.08**	**-0.60**	**0.75**	**-0.80**	**-0.37**	**0.80**	**0.83**	**0.77**	**0.63**	**0.16**	**0.28**	**0.18**	**0.15**	**0.49**	**-0.86**	**1.00**	-	-
TSR (3500)	**-0.13**	**0.08**	**-0.68**	**0.88**	**0.03**	**-0.49**	**0.81**	**-0.68**	**-0.22**	**0.86**	**0.86**	**0.83**	**0.62**	**0.31**	**0.44**	**0.31**	**0.05**	**0.72**	**-0.79**	**0.90**	**1.00**	-
OT % Load Reduction (2000 cycles)	**0.11**	**-0.28**	**0.75**	**-0.98**	**-0.17**	**0.44**	**-0.81**	**0.62**	**0.55**	**-0.82**	**-0.79**	**-0.76**	**-0.55**	**-0.48**	**-0.61**	**-0.50**	**0.01**	**-0.47**	**0.83**	**-0.89**	**-0.86**	**1.00**

To highlight a few of the key results from the Pearson correlation, a strong relationship exists between the overlay tester results and several volumetric properties including asphalt content (AC), nominal maximum aggregate size (NMAS), voids in mineral aggregate (VMA), percent passing #4 and #200 and surface area (SA). OT is also strongly correlated with IDT results from dry testing condition and TSR results after 500 and 3500 conditioning cycles. TSR results after both 500 and 3500 conditioning cycles showed a strong correlation for AC, VMA, percent passing #4 and #200 and SA. It is also not surprising that TSR results after 500 cycles and 3500 cycles are strongly correlated with each other as they are evaluating similar performance characteristics but simply different conditioning durations.

There was no significant correlation observed between PG low temperature (PGLT), or useful temperature interval (UTI), which is the difference between PG high and PG low temperatures. Also, RDCI has a perfect correlation (value of 1) between CRI and FI, which is not surprising since they are related to each other and are calculated using same test results. Among all the performance test included in the statistical analysis, OT shows the most sensitivity with respect to volumetric properties and other performance tests.

4.2 Lab Performance Compared to Volumetric Properties

To evaluate the relationship between lab performance tests to volumetric properties, DCT, SCB and OT test results were selected to be investigated further. For demonstration purposes, asphalt content and NMAS were selected as volumetric properties to be plotted against DCT, SCB and OT results. Figure 26 shows the relationship between fracture energy and fracture strain tolerance determined from DCT testing with respect to asphalt content.

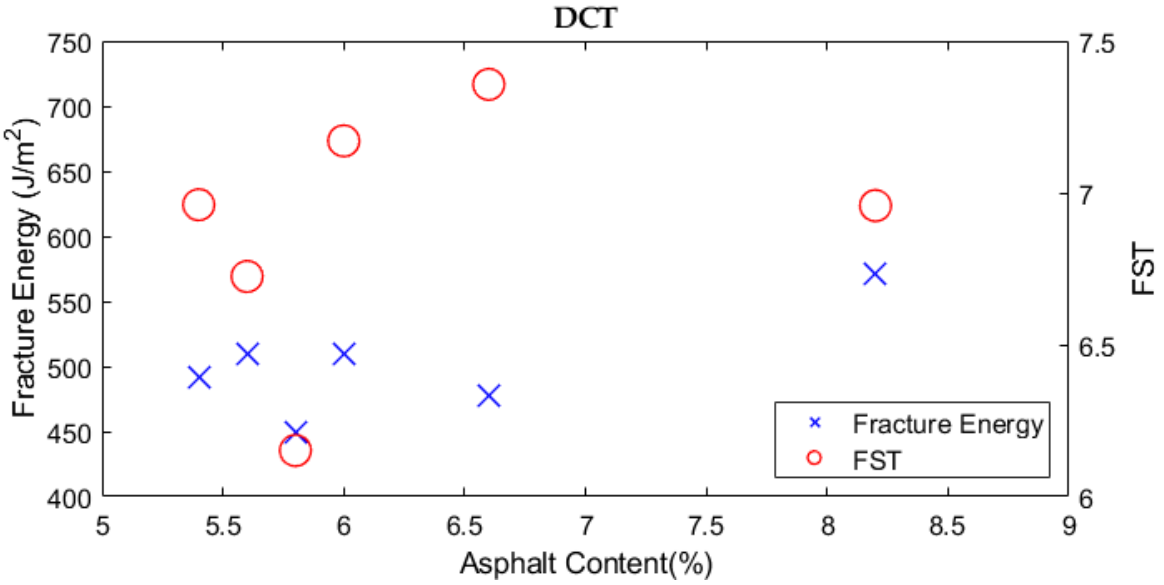

Figure 26:DCT performance indices versus asphalt content.

Figure 27 shows the relationship between FI, RDCI and CRI with respect to asphalt content. It is expected that as asphalt content increases the performance of mixtures increases for all three indices.

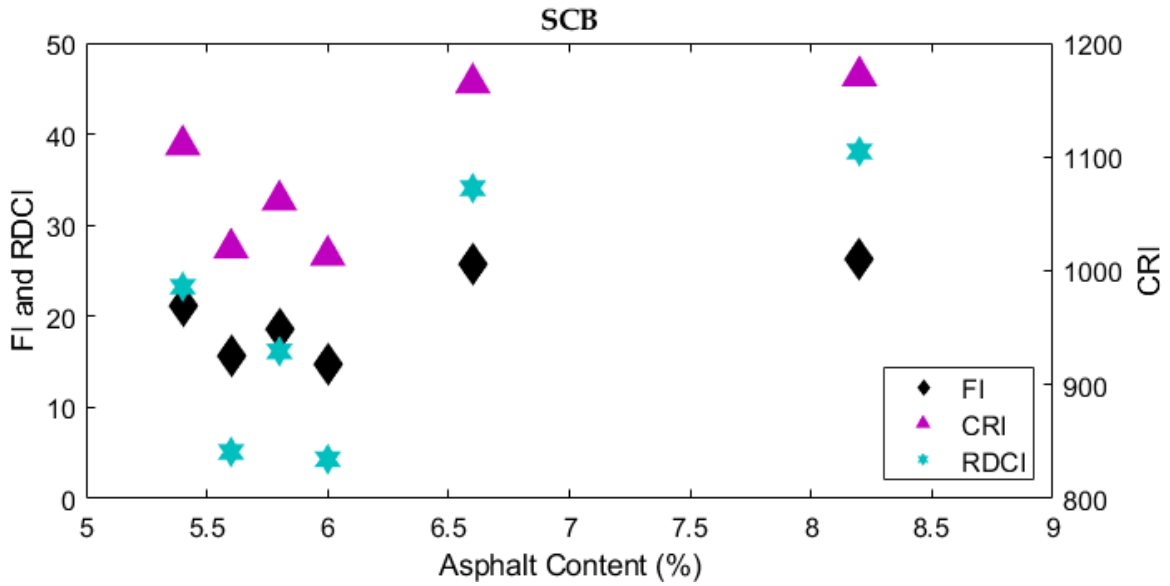

Figure 27: SCB performance indices versus asphalt content.

Two different points of interest from the overlay tester were plotted with respect to asphalt content, the number of cycles at 93% load reduction and the load reduction value at 1000 cycles. A higher number of cycles at 93% reduction is desirable and a lower load reduction at 1000 cycles indicates better cracking resistance. A relatively linear increase in the number of cycles at 93% load reduction is observed as asphalt content increases. This trend makes sense as the percentage of asphalt content increase typically corresponds to an increase in cracking resistance.

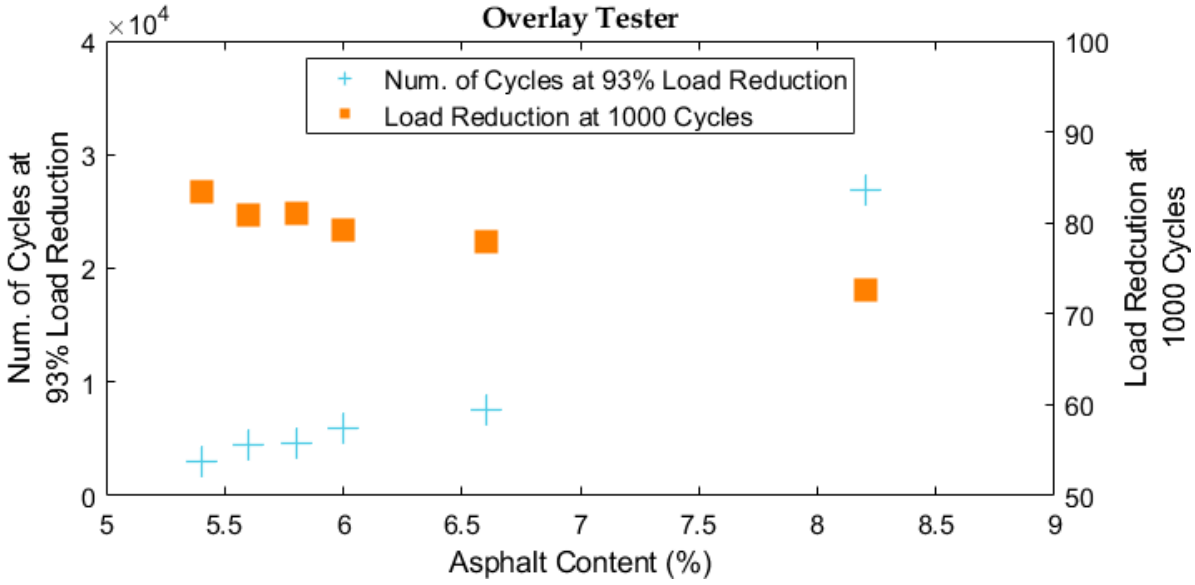

Figure 28: Overlay tester performance indices versus asphalt content.

The same performance indices from DCT, SCB and OT testing were plotted with respect to NMAS to identify any relationships among lab testing and performance. There was no significant trend in performance from DCT testing with respect to NMAS as shown in Figure 29.

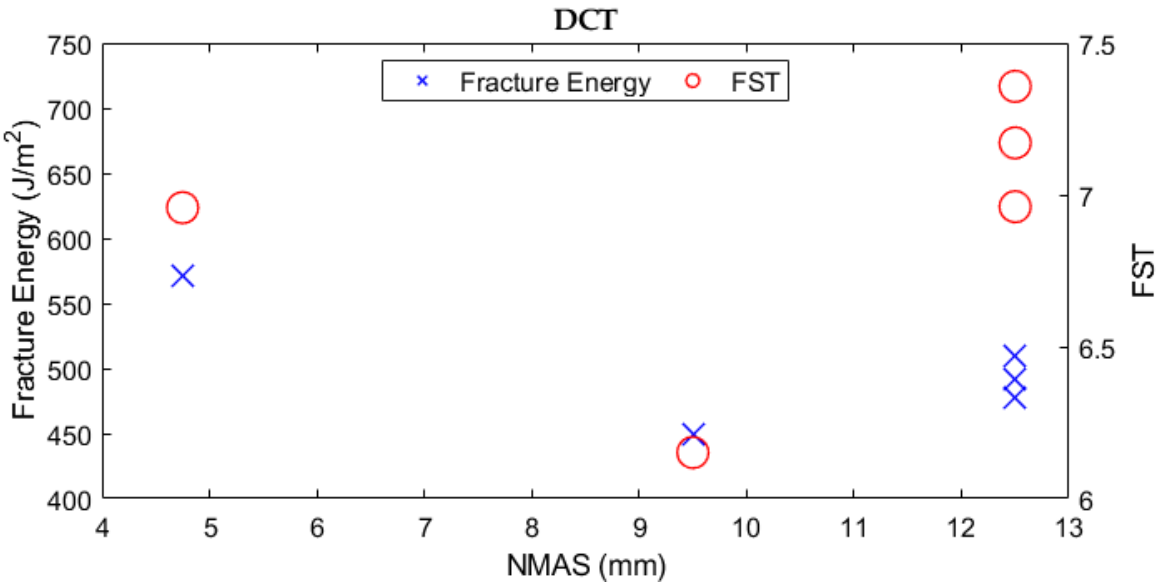

Figure 29: DCT performance indices versus NMAS.

A slight decrease in SCB performance results is observed as the NMAS increases (Figure 30). This trend also makes sense because mixtures with lower NMAS contain higher amounts of asphalt content (Table 2), which helps to improve fatigue cracking resistance.

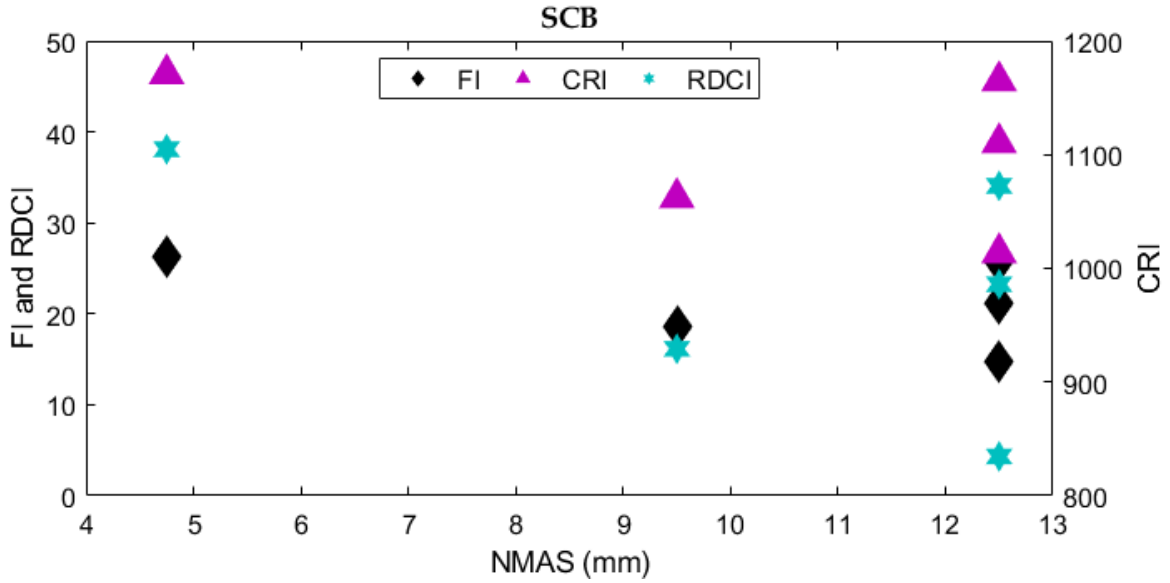

Figure 30: SCB performance indices versus NMAS.

Lastly, OT results were plotted with respect to NMAS in Figure 31. A positive linear increasing trend in load reduction at 1000 cycles results as NMAS size increases. In comparison, the number of cycles at 93% load reduction decreases linearly with an increase in NMAS size.

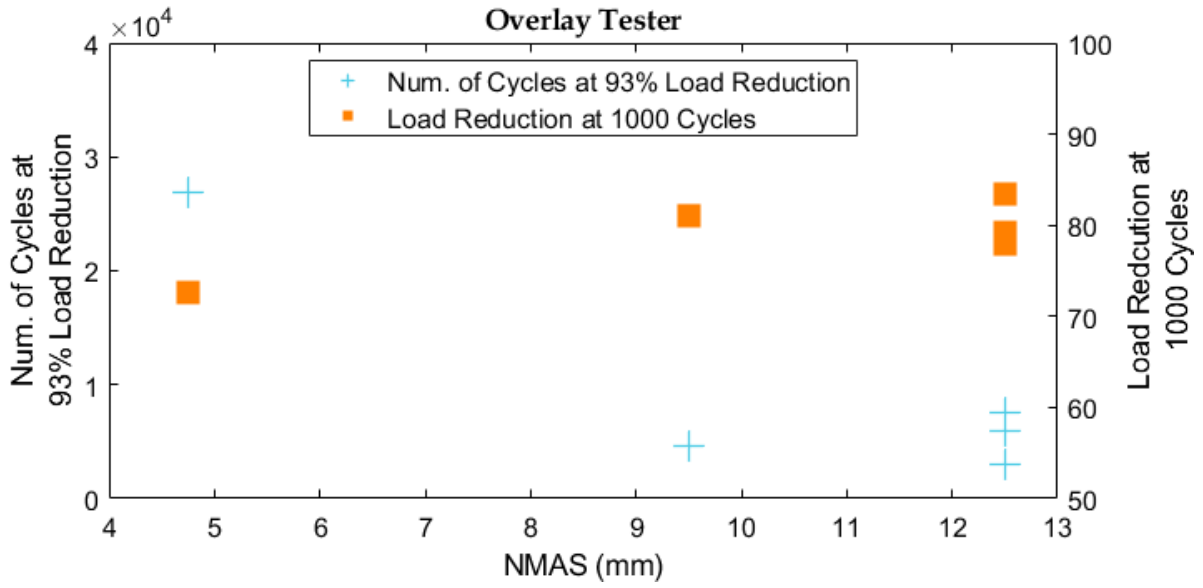

Figure 31: Overlay tester performance indices versus NMAS.

4.3 Lab Performance Compared to Field Performance

Lab performance data from DCT, SCB and OT was compared to field performance data in the form of percent cracking located at joints for all surface course mixtures. Distress crack maps were used to quantify the percent of joints cracked within each test cell section and that value was then assigned to the surface course within that test section. While this is a simplification and does not account for the overall structure of each test section, it provides a preliminary method to estimate the correlation of lab performance tests with field performance. Figure 32 shows that there is no strong correlation between FE or FST with field performance data. A slight decrease in FST is observed as the percent cracking at joints increases.

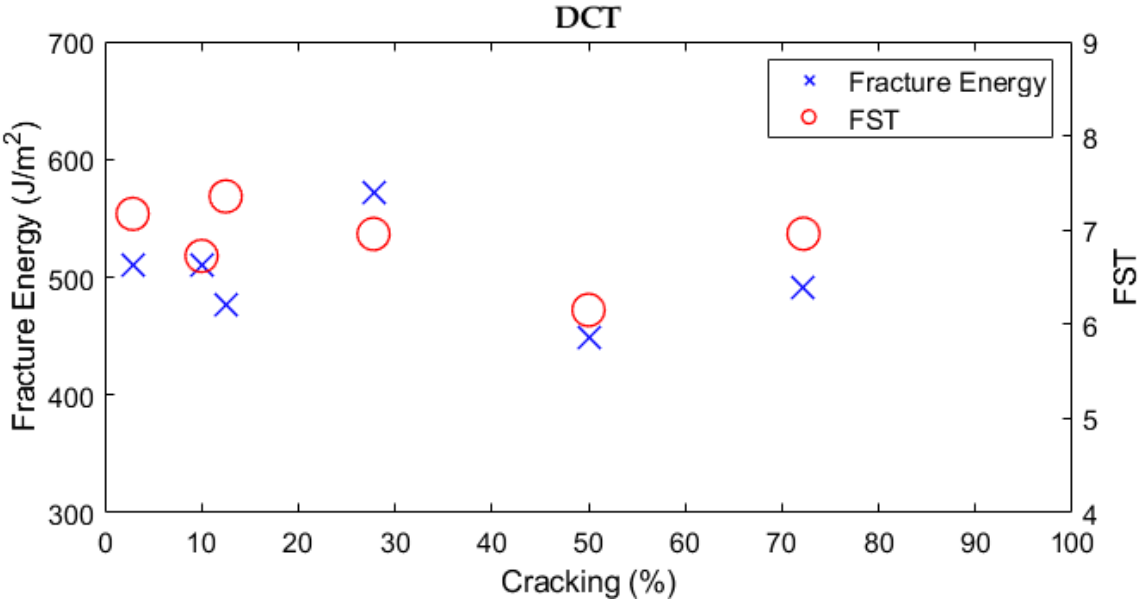

Figure 32: DCT performance indices versus percent cracking at joints after 1 year of placement.

Similarly to DCT performance indices, there was no significant trend observed when comparing SCB performance indices FI, RDCI or CRI with field performance cracking data (Figure 33).

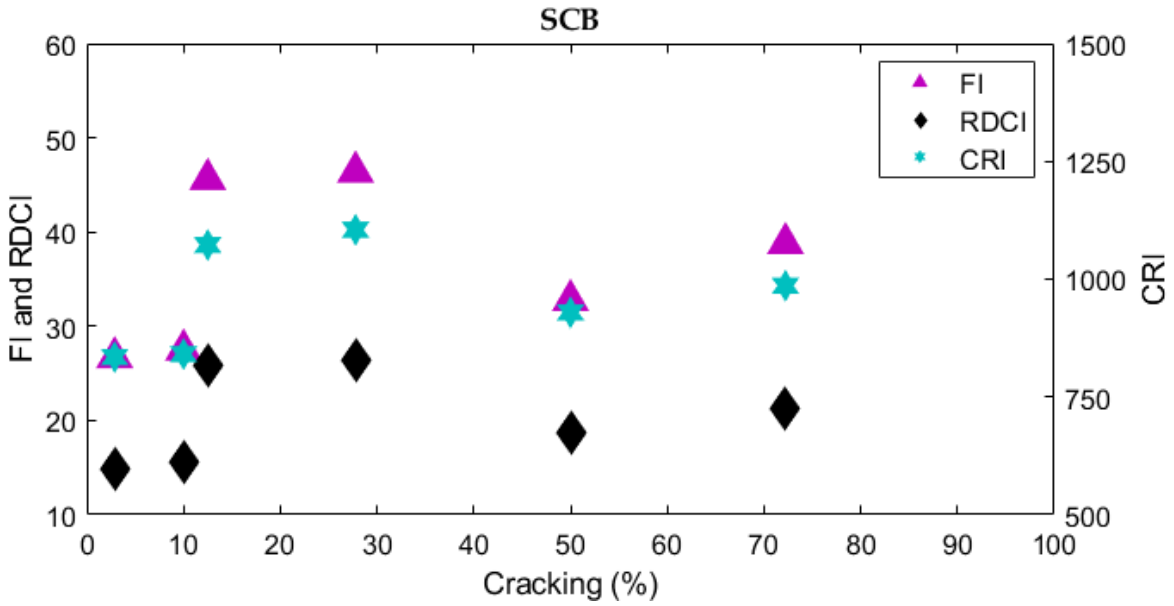

Figure 33: SCB performance indices versus percent cracking at joints after 1 year of placement.

Figure 34 shows no conclusive correlation of OT lab testing with field performance. It is hypothesized that with more time in the field a stronger correlation may develop among lab performance tests and field performance data.

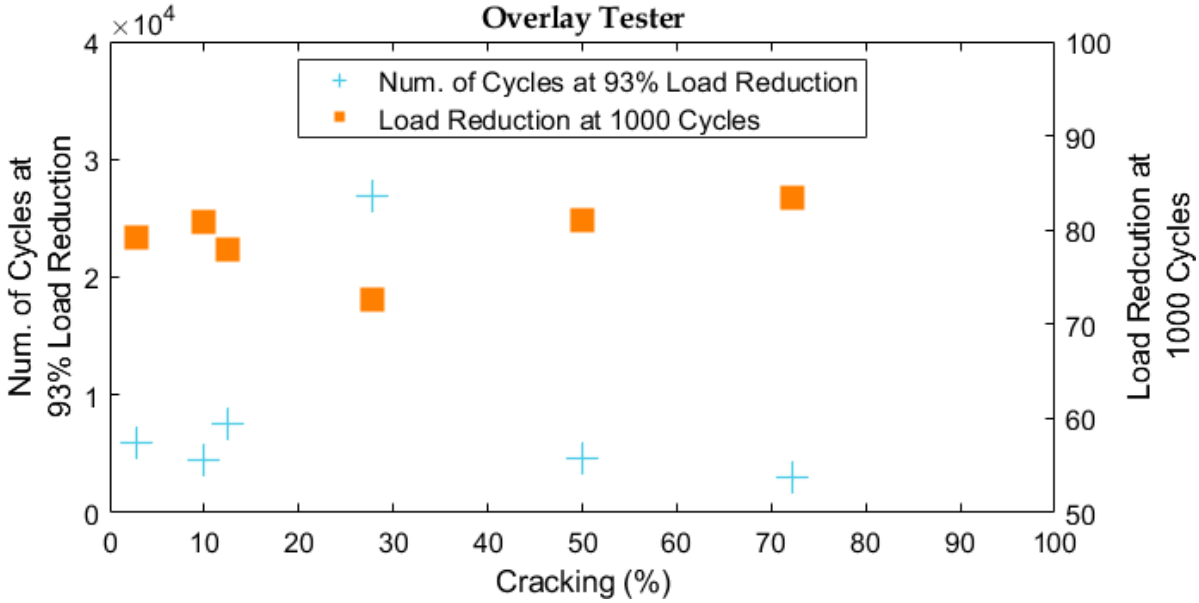

Figure 34: OT performance indices versus percent cracking at joints after 1 year of placement.

5. Survey Results

A survey was developed by the UNH research team and distributed to all six NRRA state members to collect information as well as data regarding HMA overlays on PCC pavements. An effort was made to collect information on performance data for first time overlays as well as subsequent overlays on PCC pavements. The survey was broken into four main components to collect information on the overlay decision process, performance data, cost data and finally contact information to send follow up surveys.

The first main question focused on determining what approaches are used to decide when an asphalt concrete overlay is warranted as a rehabilitation treatment. Currently, standard policy is the most common method of deciding when an asphalt overlay is used as a rehabilitation option for PCC pavements (Figure 35). Decision tree tools are currently only being used by MnDOT and CalTrans, while Illinois Department of Transportation (IDOT) is currently in the process of developing a decision tree tool for their department.

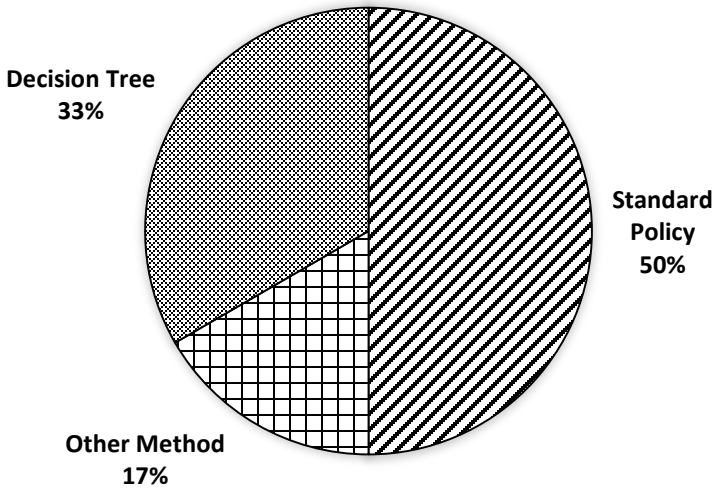

Figure 35: Rehabilitation of asphalt concrete overlays tools or methods used by NRRA state members.

After determining which mechanism is most popular, researchers also wanted to determine which inputs and outputs are involved in the decision making process. Among all state responses, common inputs in the decision making process included design life, traffic level, current condition of pavement, IRI, past experience, cost and availability of funding. In comparison, the outputs from the decision making process varied slightly state by state. For example, Michigan Department of Transportation (MDOT) considers first if the overlay will be cost effective, and then determines how many courses of HMA should be used based on judgement and past experience. Meanwhile, IDOT uses HMA overlay thickness set by a standard policy (53-4.07) unless an exception is granted, often in combination with PCC patching prior to HMA overlay. Wisconsin Department of Transportation (WisDOT) uses an approach similar to IDOT, whereby PCC patching and repair is done in combination with HMA overlay but a pavement engineer determines the thickness and design of overlay using WisPAVE or ME.

The next portion of the survey focused on determining the availability of performance data of asphalt concrete overlays from the NRRA states. While 4 out of the 6 states have conducted a pavement performance study on asphalt overlays on PCC pavements, only three states are able to share data sets and or published reports. Only IDOT has performed laboratory testing as part of a pavement performance study on asphalt overlays on PCC pavements. For further details, FHWA-ICT-17-020 report may be consulted.

Five out of six states agencies have conducted or participated in data gathering and analysis efforts to determine service life and reflective cracking performance of asphalt overlays on PCC pavements. In general, distress maps, visual surveys and the use of van videotapes on pavement surfaces were common methods to collect data.

In terms of measuring in-situ performance data, International Roughness Index (IRI) was the most popular method with 50% of NRRA members using this method. Other methods used to assess in-situ performance include PASER Rating, Distress Index (DI) (which is a measure that is an accumulation of points for observed distresses) and falling weight deflectometers. However, it should be noted that only one state has both performance data and in-situ density measurements available. An effort will be made in follow up surreys to collect in-situ density data as well as performance data from the NRRA state members in order to draw comparisons between past data and the current MnROAD study.

Lastly, the accessibility of cost data was evaluated among the NRRA members. Four out of six states reported that cost data for asphalt overlay designs on PCC pavements is available. Examples of cost data to collected in the follow up survey include project planning cost estimates, design package cost estimates, recent construction project costs and unit prices for HMA from individual construction projects. Contact information was collected from those states that were able to provide cost data and will be used to distribute a follow up survey in the near future.

6. Summary

In fulfillment of Task-2, a summary of lab test results and field performance data was presented. Statistical comparison by means of Pearson correlation was performed on volumetric properties as well as lab performance data. Results from the NRRA state member survey was summarized and a follow up survey to obtain cost data will be sent out to state members in the upcoming future. It should be noted that two test results were not included in the Task-2 deliverable. Simplified viscoelastic continuum damage (S-VECD) and compact tension (CT) test were not included due to a test equipment mechanical issue that has delayed the completion of testing. Once the issue is resolved, S-VECD and CT results will be submitted in a follow up memo to the Task-2 deliverable. Lastly, a continued effort to analyze in-situ performance data will be conducted as data becomes available (e.g. rolling density measurements (RDM) and cores).

As more field performance results are made available to the research team, trends between performance tests and field performance are becoming clearer. The latest field results from April, 2019, are providing helpful insight into the difference between short term and long term field cracking performance. Investigation of additional field cracking performance indices is underway by the research team to assess and compare different overlay pavement structures while taking into account time in service.

7. References

Al-Qadi, Imad L., et al. *Utilizing Lab Tests to Predict Asphalt Concrete Overlay Performance*. Illinois Center for Transportation/Illinois Department of Transportation, 2017. http://hdl.handle.net/2142/98920

F. Yin, E. Arambula, R. Lytton, Epps Martin, A., Garcia Cucalon, L. Novel Method for Moisture Susceptibility and Rutting Evaluation Using Hamburg Wheel Tracking Test. In Transportation Research Record 2446, TRB, National Research Council, Washington, D. C., 2014, pp. 1-7.

Kaseer, Fawaz, et al. "Development of an index to evaluate the cracking potential of asphalt mixtures using the semi-circular bending test." Construction and Building Materials 167 (2018): 286-298.

Nemati, R., Haslett, K., Dave, E. V., Sias, J." Development of a Rate-Dependent Instantaneous Power based Cracking Index Parameter for Asphalt Mixtures", Under Publication, Road Materials and Pavement Design. 2019

Van Deusen, Dave, et al. *Report on 2017 MnROAD Construction Activities*. Minnesota Department of Transportation. Report Number: MN/RC 2018-16. 2018. www.dot.state.mn.us/mnroad/nrra/documents/2017 Construction Report.pdf.

Zhu, Yuefeng, et al. "Comprehensive evaluation of low-temperature fracture indices for asphalt mixtures." Road Materials and Pavement Design 18.sup4 (2017): 467-490.

8. Appendix

A.1 Hamburg Wheel Tracker (HWT)

Following the TTI method to analyze rutting and stripping susceptibility, when mixtures do not contain an inflection point, the stripping number and stripping life cannot be determined. To demonstrate this difference, Figures 35 and 36 show the determination of the stripping number and stripping life for SPWEA440E mixture (does not have an inflection point), and Figure 37 and 38 show the determination of stripping number and stripping life for SPWEB400E (has an inflection point).

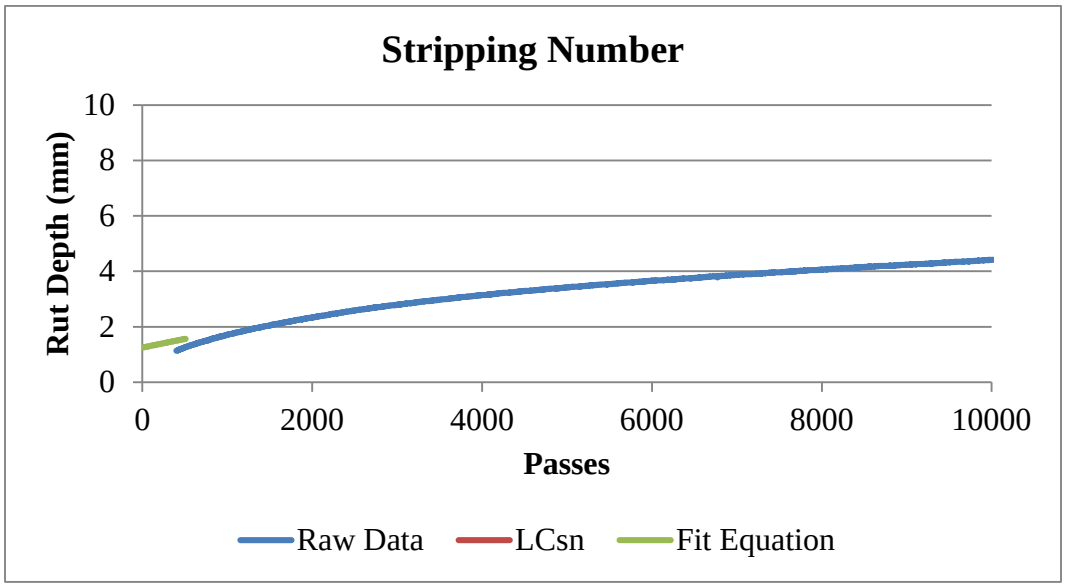

Figure 36: Stripping number determination for SPWEA440E mixture.

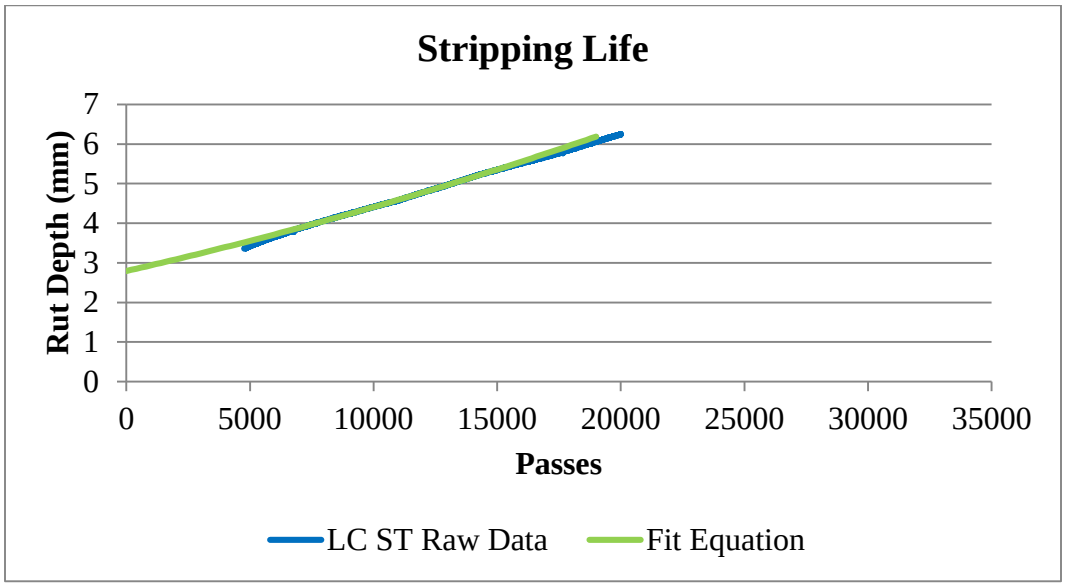

Figure 37: Stripping life determination for SPWEA440E mixture.

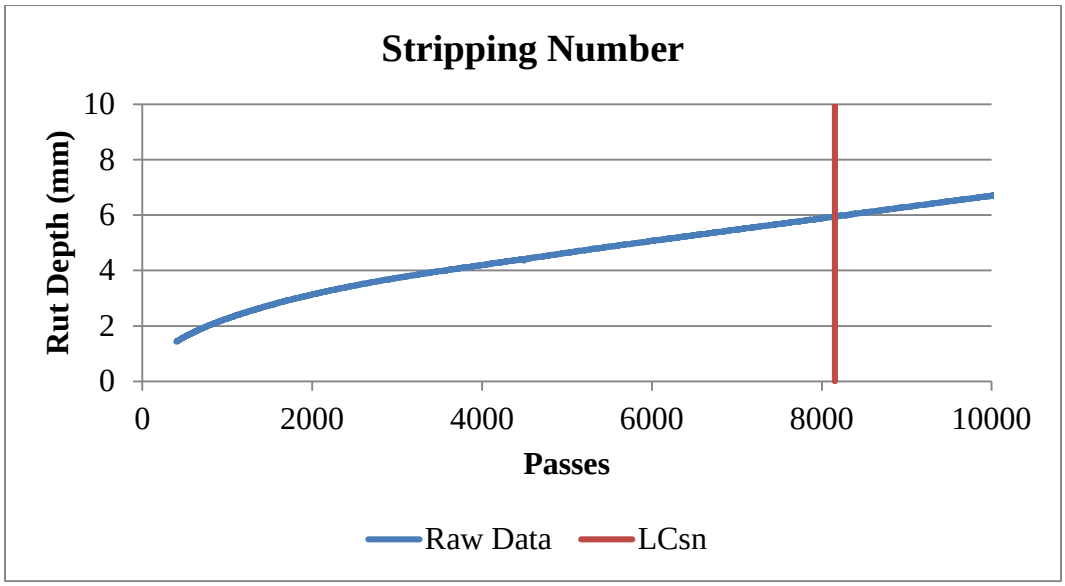

Figure 38: Stripping number determination for SPWEB440E mixture.

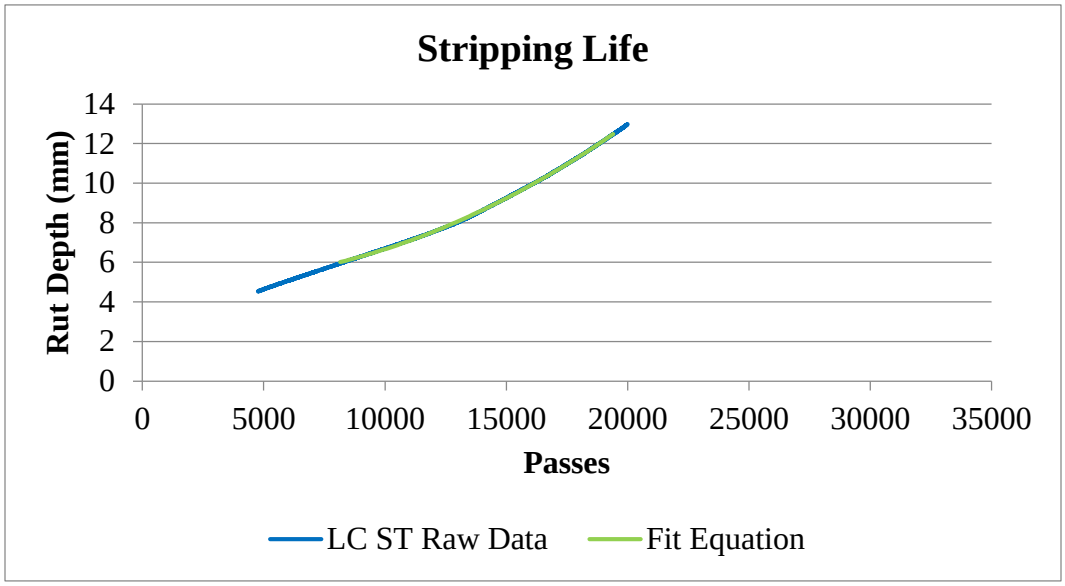

Figure 39:Stripping life determination for SPWEB440E mixture.